CrossMark

Pricing VIX derivatives with free stochastic volatility model

Wei Lin[1] · **Shenghong Li[1]** · **Shane Chern[2]** · **Jin E. Zhang[3]**

Abstract This paper aims to develop a new free stochastic volatility model, joint with jumps. By freeing the power parameter of instantaneous variance, this paper takes Heston model and 3/2 model for special examples, and extends the generalizability. This model is named after free stochastic volatility model, and it owns two distinctive features. First of all, the power parameter is not constrained, so as to enable the data to voice its authentic direction. The Generalized Methods of Moments suggest that the purpose of this newly-added parameter is to create various volatility fluctuations observed in financial market. Secondly, even upward and downward jumps are separately modeled to accommodate the market data, this paper still provides the quasi-closed-form solutions for futures and option prices. Consequently, the model is novel and highly tractable. Here, it should be noted that the data on VIX futures and corresponding option contracts is employed to evaluate the model, in terms of its pricing and implied volatility features capturing performance. To sum up, the free stochastic volatility model with asymmetric jumps is capable of adequately capturing the implied volatility dynamics. Thus, it can be regarded as a model advantageous in pricing VIX derivatives with fixed power volatility models.

Keywords Free stochastic volatility · Jumps · VIX derivatives

JEL Classification G13

✉ Wei Lin
 weilin1991@zju.edu.cn

1 School of Mathematical Sciences, Zhejiang University, Hangzhou 310000, China

2 Pennsylvania State University, State College, USA

3 Department of Accountancy and Finance, University of Otago, Dunedin, New Zealand

🖄 Springer

1 Introduction

The trading volume of derivatives on the VIX index has experienced considerable growth, acquiring measurable prevalence among investors, since Chicago Board Options Exchange (CBOE) launched the CBOE Volatility Index (VIX) futures in March 2004, together with the later release of VIX options in February 2006 and a great deal of financial innovation in volatility traded on markets over the past decade. And this increasing volume shall attribute to the fact that VIX options give investors the possibility to directly and effectively invest in volatility, unnecessary to factor in the price changes of the underlying instrument, dividends, interest rate or expiration date. Moreover, VIX derivatives can serve as an effective hedging instrument against financial turmoil. In fact, the index is regarded as the "fear gauge" since the rise in VIX index mirrors an incoming large price movement and market turmoil, whereas the low and steady status in VIX index usually refers to an easing upward in a long-run bull market.

In this paper, we coin the term *free stochastic volatility* to describe the fact that the volatility of the VIX is not merely stochastic but also varies asymmetrically in response to changes in the S&P500. The dynamics of the VIX and the VVIX in the CBOE could be taken for a very example for such asymmetry. The aforementioned VIX and VVIX not only fluctuate, randomly and frequently, but also change asymmetrically, upward and downward. Simultaneously, an interesting point of empirical regularity is that the stochastic volatility of the VIX mainly derives from two components—one can be spanned by S&P500 while the other one cannot. In order to determine the precise extent to which VIX can be influenced by S&P500, we run a regression of S&P500 returns onto VIX returns, finding that the S&P500 changes can explain 69% of the variation in the VIX based on the adjusted R^2 of the regression, which means that modeling the dynamics of S&P500 returns becomes extremely essential prior to VIX derivatives pricing. Thus, a consideration of free stochastic volatility is expected to better capture the dynamics of S&P500 returns, which in turn better reconciles the theoretical model with VIX. As a result, option valuation is improved. Figure 1a, b depict the historical dynamics of the VIX index, along with its volatility VVIX index and S&P500 index respectively. Figure 1c also presents a scatter plot of VIX returns against S&P500 returns. Inspection of Fig. 1, a number of important features need to be addressed here if one desires to jointly model the S&P500 and VIX dynamic. Firstly, there is a positive relation between changes in VVIX and VIX. Secondly, the time-variated VIX fluctuation shows the respective high and low volatility period. Besides, the time-variated VIX fluctuation presents a fairly stochastic feature which calls for the demand for freeing volatility models capable of flexibly reproducing the observed volatility. Last but not least, the S&P500 and VIX index are negatively correlated, i.e. the leverage effect, meanwhile there are also signs of simultaneously and oppositely directed jumps between S&P500 and the VIX index.

In contrast to the aforementioned empirical fact, the existing VIX-option-themed papers generally assume that the power of instantaneous variance in S&P500 follows either square root or 3/2. Based on Heston (1993) model, Grunbichler and Longstaff (1996) priced options on instantaneous volatility, letting the volatility process follow a mean-reverting squared Bessel process (usually called CIR or square root process
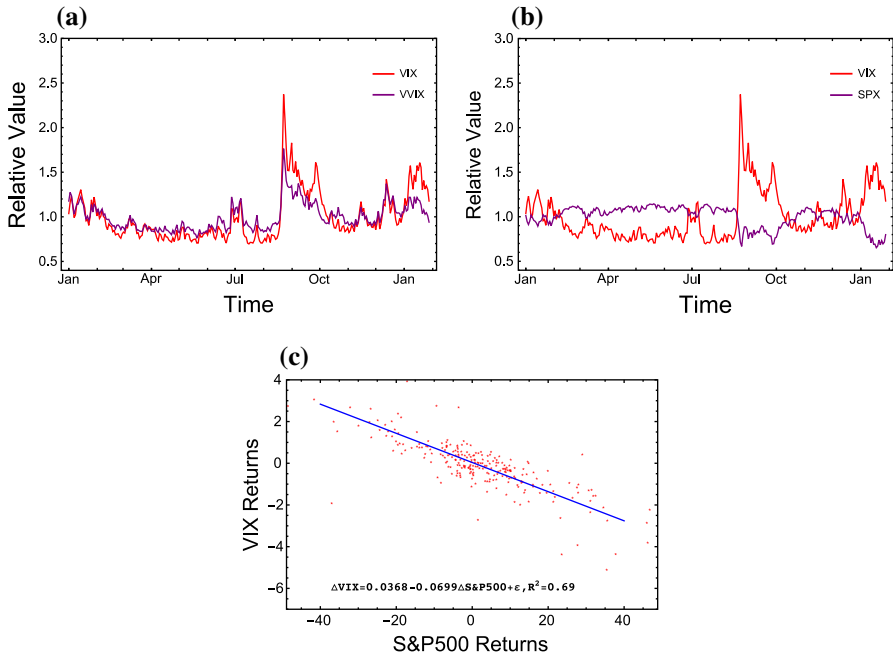
Fig. 1 Plot of the VIX index against S&P500 and VVIX(01/02/2015–1/29/2016). **a** VVIX versus VIX, **b** S&P500 versus VIX, **c** Scatter plot of VIX returns versus S&P500 returns

since it displays a power 1/2 in the diffusion term). Later, Zhang and Zhu (2006) proposed VIX futures pricing. Lian and Zhu (2013) extended this to the case of VIX options in which the underlying index and its volatility are allowed to jump. Thereafter, the inverse of CIR process is mean-reverting as well, and the power of its diffusion term is 3/2. The relevant paper written by Drimus (2012) researched on the pricing and hedging of options on realized variance in the 3/2 non-affine model. Later, in a 3/2 stochastic volatility model with jumps in the underlying index, Baldeaux and Badran (2014) derived a semi-closed formula for VIX options. Here is an interesting point that Duan and Yeh (2010) introduced a joint price-volatility model which is more general than that of Bate (Bates 2000) and Pan (2002) due to its free-root in volatility process. In Lin et al. (2017), empirical analysis concluded that the assumption on which previous models are built that the volatility diffusion term in equity is either square root or 3/2 fails to underpin the accurate accommodation of important feature of the VIX data and volatility skew. What is more, a new 4/2 model is proposed in their paper as the superposition of 1/2 and 3/2 terms to overcome the respective disadvantages. The volatility diffusion term in equity of those models is a fixed power of CIR process, i.e. 1/2, 3/2 or 4/2. Hence, we free rather than setting limitations to stochastic volatility parameter α to be the power of instantaneous variance, allowing the data to voice its authentic direction. Therefore, this model is named after free stochastic volatility model (FSV), and this paper aims to demonstrate the capacity of pricing VIX derivatives with FSV model so as to bridge the literature gap.

The purpose of this paper is threefold. Firstly, we built non-jump FSV model and addressed a couple of technical conditions to avoid a well-defined FSV model's possible explosion. Under this framework, this new stochastic volatility model takes both Heston (1993) and 3/2 model (Baldeaux and Badran 2014) for special examples, so as to embrace a greater control over the distribution shape of asset returns. Unlike the four-parameter stochastic processes, the Heston and 3/2, the additional fifth parameter α of the new process is expected to flexibly capture and control the distribution of logarithm stock return. From this perspective, the estimation technique Generalized Methods of Moments (GMM) of Hansen (1982) is outlined to empirically estimate and compare these models. GMM is first introduced by Chan et al. (1992) to compare the short-term interest rate models. Later, Goard and Mazur (2013) used this method to compare different models which describe VIX but do not provide a connection to the underlying index. In comparison to Goard and Mazur's direct application of GMM, our determinative difference lies in providing a connection to the dynamic of the underlying index, especially in aspects of arbitrage assumptions and the way that models are used in practices. Then, the second determinative difference is that we have done the estimation exercises for four different times, in order to assess whether FSV parameter α changes significantly in parallel with time. We ended in drawing conclusion that α implies different volatility fluctuations in different periods, and should be taken into consideration in our model.

Secondly, we established FSV model with respective upward and downward setting, both of which are assumed to follow independent compound Poisson processes while each has its own jump intensity and exponential jump-size distribution. Although Park (2016) proposed this kind of asymmetric jumps in his model, Park only added these two jumps in the dynamics of the VIX, without providing underlying index. Back to our model, we established upward and downward jumps in underlying index. Following Lewis (2000, Chapter 9), in economically reasonable stochastic volatility models, the actual volatility should be a recurrent process without explosion. An explosion in the auxiliary volatility process causes some discounted financial claim prices to fail to be martingale; instead, they are local martingales only. In light of these claims, we proposed and proved that the discounted stock price is more than a local martingale under our FSV model, but a true martingale.

Thirdly, we introduced four models of S&P500 price dynamics of which the differences are decided whether models contain the free stochastic volatility α and jumps. Each model can derive its quasi-analytic solutions for future and option prices. The first one is the stochastic volatility (HSV) model built on Heston model (Heston 1993). The second one is the 3/2 stochastic volatility plus jumps (3/2-SVJ) model provided by Baldeaux and Badran (2014). The following two models (FSV-type) free the power parameter of instantaneous variance: the third model is the FSV model with asymmetric jumps (FSV-AJ), which represents that upward and downward jumps are both assumed to follow independent compound Poisson processes while each has its own jump intensity and exponential jump-size distribution. The forth model is the FSV model with downward jumps only (FSV-DJ), in order to compare FSV-AJ and investigate whether upward jumps can have an incremental effect on the pricing of VIX derivatives. These consistent models contain information about S&P500 index, VIX

index, VIX futures and VIX options. Hence, models are tested on the foregoing data covering span between March 1, 2016 and March 31, 2016.

Our paper investigates the effects of FSV parameter α on the pricing of VIX derivatives. By comparing the FSV-type with 3/2-SVJ and HSV, we found that the former is strongly and obviously preferable to the latter, in terms of the in-sample and out-of-sample testing results. Then, by comparing FSV-DJ and FSV-AJ model, the in-sample and out-of-sample tests show that FSV-AJ slightly outweighs FSV-DJ, more apparently in OTM options. We plot the VIX futures values as a function of time to maturities under four models, and present in Fig. 4. In addition, we plot those of the VIX option values as a function of strikes, presented in Fig. 5. Thereafter, we concluded that acceptance for FSV parameter α in model makes large improvements in fitting the prices of VIX futures and options. Subsequently, we eyed on the respective effects of setting upward and downward jumps. Good and bad surprises may arrive with different rates and sizes and investors may react differently to them. Hence, our models assume that upward and downward jumps occur independently with different frequencies and magnitudes. Results show that including upward jump contributes to OTM options pricing. We ended in finding that a joint consideration of the FSV parameter α and asymmetric jumps is expected to better capture the dynamics of equity returns, which in turn better reconciles the theoretical model with the observed volatility smile/smirk. As a result, valuation of VIX futures and options is improved.

It should be mentioned that the ability of FSV-type models (FSV-AJ and FSV-DJ) to match S&P500 options remains unknown, as it involves a problem of computing an expectation which exceeds the known results on CIR. The unsolved expectation is $\mathbb{E}_t \left[\exp \left(\int_t^T V_t^\alpha dt \right) \right]$ where V_t is CIR process and $\alpha \in \mathbb{R}$. According to Grasselli (2017), this expectation can be solved only with special values of α, such as $\alpha = 1$ or -1. We hope that our future work can concentrate on this unsolved expectation. Fortunately, we found that FSV-type models can price VIX derivatives directly. Repeatedly, exploring the possibility and effectiveness for pricing VIX derivatives in these models are the very purposes of this paper.

As the volatility of S&P500, the sole modeling VIX without providing the dynamics of S&P500 is far from being self-proved and reasonable. In accordance with Fig. 1c, the adjusted R^2 of the regression explains that the dynamics of S&P500 returns can not be rejected in modeling VIX. Thus, a consideration of free stochastic volatility is expected to better capture the dynamics of S&P500 returns. This means that our approach is superior to an approach in which the dynamics of the VIX are model directly (Goard and Mazur 2013).

The balance of this paper is organized as follows. In Sect. 2, we proposed FSV model under physical probability measure and its non-explosion condition, together with estimation technique, GMM, outlined in empirical test. In Sect. 3, we presented the general FSV-AJ model setup and proved that the discounted stock price is a martingale, under risk-neutral measure. In Sect. 4, both pricing formulas of VIX future and option are provided, and the relevant data are described in Sect. 5. Section 6 shows the parameters estimation and some preliminary analysis, while Sect. 7 provides the main empirical result on pricing performance beyond the different model specifications. Concluding remarks are offered in Sect. 8.

2 Free stochastic volatility model applied to the S&P500

In this section, consider a given filtered complete probability space $(\Omega, \mathscr{F}, \mathbb{P})$ and information filtration $\{\mathscr{F}_t\}_{t\geq0}$ where the price process S_t is adapted to the filtration $\{\mathscr{F}_t\}_{t\geq0}$. The statistical dynamics for stock price and variance process include free stochastic volatility parameter α and Cox–Ingersoll–Ross (CIR) process:

$$\frac{dS_t}{S_t} = \left(r + \delta_s^* V_t\right) dt + \gamma^* V_t^\alpha dW_t^\mathbb{P}, \tag{2.1}$$

where the stochastic factor V evolves as

$$dV_t = \kappa^* \left(\theta^* - V_t\right) dt + \sigma\sqrt{V_t} dZ_t^\mathbb{P}, \tag{2.2}$$

starting at $S_0 > 0$ and $V_0 > 0$, respectively. As usual, r, κ^* and θ^* are assumed to be strictly positive. θ^* controls for the long-term mean of V_t, while κ^* is the mean-reversion speed of V_t. Furthermore, $\sigma \in \mathbb{R}$ captures the volatility of V_t and $\delta_s^* \in \mathbb{R}$ stands for asset risk premium. $W_t^\mathbb{P}$ and $Z_t^\mathbb{P}$ are standard Brownian motions under $\mathbb{P}$ measure. $\alpha \in [-\frac{1}{2}, \frac{3}{2}]$ represents the free stochastic volatility part so we hope it can capture more complicated fluctuations of volatility implied in S&P500. Then, $dZ_t^\mathbb{P}$ and $dW_t^\mathbb{P}$ are two correlated Wiener processes with the correlation coefficient equal to $\rho \in [-1, 1]$. Giving credits to the characteristic that specifications correspond to the special case of a fixed α, our joint price-volatility model demonstrates a better generalizability in comparison to Heston model and 3/2 stochastic model.

Now technical conditions should be addressed so as to make the free stochastic volatility model well-defined. Then, in order to avoid the possible V_t^α explosion, some technical conditions upon parameters should be satisfied. First, apply the Itô formula to $D_t = V_t^\alpha$, so we get

$$dD_t = \left(\alpha D_t^{1-\frac{1}{\alpha}} \left(\kappa^*\theta^* + (\alpha - 1)\frac{\sigma^2}{2}\right) - \alpha\kappa^* D_t\right) dt + \alpha\sigma D_t^{1-\frac{1}{2\alpha}} dZ_t^\mathbb{P}.$$

Its scale density is

$$s(D) = D^{-\frac{2\tilde{\theta}}{\alpha\sigma^2}} e^{\frac{2\kappa^*}{\sigma^2} D^{\frac{1}{\alpha}}},$$

where $\tilde{\theta} = \kappa^*\theta^* + (\alpha - 1)\frac{\sigma^2}{2}$. Hence, the scale measure $S(c, d)$ becomes

$$S(c, d) = \int_c^d s(x)dx = \int_c^d x^{-\frac{2\tilde{\theta}}{\alpha\sigma^2}} e^{\frac{2\kappa^*}{\sigma^2} x^{\frac{1}{\alpha}}} dx.$$

In particular, we see that

$$S(c, +\infty) \begin{cases} = \infty & \text{for (i) } \alpha > 0 \text{ or (ii) } \alpha < 0 \text{ and } \tilde{\theta} > 0, \\ < \infty & \text{for } \alpha < 0 \text{ and } \frac{2\tilde{\theta}}{\alpha\sigma^2} > 1. \end{cases} \tag{2.3}$$

Thus, if $\tilde{\theta} > 0$, $S(c, +\infty)$ can totally be divergent, regardless of the value of α. Following the boundary classification criteria mentioned in Lewis (Lewis 2000, Table 9.2), $D = \infty$ is classified as a natural or entrance boundary. Fortunately, either of these two boundaries makes $D = \infty$ unreachable from the interior in finite time, which means that $D = V_t^\alpha$ never explodes in finite time.

Furthermore, CIR process is a space-time change BESQ process. Applying Feller's boundary condition, V_t process starting from a positive initial point stays strictly positive and never explodes in finite interval, if and only if $2\kappa^*\theta^* \geq \sigma^2$. In order to avoid the possible explosion of V_t and V_t^α, $\tilde{\theta} > 0$ and $2\kappa^*\theta^* \geq \sigma^2$, i.e.

$$\frac{2\kappa^*\theta^*}{\sigma^2} > 1 - \alpha \quad \text{and} \quad \frac{2\kappa^*\theta^*}{\sigma^2} > 1$$

are established to be two technical conditions on parameters. If $\alpha > 0$, then $\frac{2\kappa^*\theta^*}{\sigma^2} > 1 > 1 - \alpha$. If $\alpha < 0$, then $\frac{2\kappa^*\theta^*}{\sigma^2} > 1 - \alpha > 1$. Leaving aside the value of α, when one technical condition is proved, the other one is self-proved simultaneously.

Before applying GMM to parameter estimation, the following Lemma 2.1 needs to be built.

Lemma 2.1 *Let* $X^x = \{X_t^x, t \geq 0\}$ *denote the solution of the (CIR) SDE in Eq.* (3.2) *and* $X_0 = x > 0$ *with* $\kappa, \theta, \sigma > 0$ *and* $2\kappa\theta \geq \sigma^2$ *(Feller condition). Consider* $\epsilon, v, \eta, \gamma \in \mathbb{R}$ *such that*

$$\epsilon > -\frac{\kappa^2}{2\sigma^2}, \tag{2.4}$$

$$v \geq -\frac{\left(\kappa\theta - \frac{\sigma^2}{2}\right)^2}{2\sigma^2}, \tag{2.5}$$

$$\eta < \frac{\kappa\theta + \frac{\sigma^2}{2} + \sqrt{\left(\kappa\theta - \frac{\sigma^2}{2}\right)^2 + 2\sigma^2 v}}{\sigma^2}, \tag{2.6}$$

$$\gamma \geq -\frac{\sqrt{\kappa^2 + 2\epsilon\sigma^2} + \kappa}{\sigma^2}. \tag{2.7}$$

The following transform for the CIR process is well defined for all $t \geq 0$ *and is given by*

$$\phi(t, x; \eta, \gamma, \epsilon, v) = \mathbb{E}\left[(X_t^x)^{-\eta} \exp\left(-\gamma X_t^x - \epsilon \int_0^t X_s^x ds - v \int_0^t \frac{ds}{X_s^x}\right)\right]$$

$$= \left(\frac{\beta(t, x)}{2}\right)^{m+1} x^{-\frac{\kappa\theta}{\sigma^2}} (\gamma + K(t))^{-\left(\frac{1}{2} + \frac{m}{2} - \eta + \frac{\kappa\theta}{\sigma^2}\right)}$$

$$\times \, e^{\frac{1}{\sigma^2}\left(\kappa^2\theta t - \sqrt{A}x \coth\left(\frac{\sqrt{A}t}{2}\right)+\kappa x\right)} \frac{\Gamma\left(\frac{1}{2}+\frac{m}{2}-\eta+\frac{\kappa\theta}{\sigma^2}\right)}{\Gamma(m+1)}$$

$$\times_1 F_1\left(\frac{1}{2}+\frac{m}{2}-\eta+\frac{\kappa\theta}{\sigma^2}, m+1, \frac{\beta(t,x)^2}{4(\gamma+K(t))}\right), \qquad (2.8)$$

with

$$m = \frac{2}{\sigma^2}\sqrt{\left(\kappa\theta-\frac{\sigma^2}{2}\right)^2 + 2\sigma^2\nu}, \qquad (2.9)$$

$$A = \kappa^2 + 2\sigma^2\epsilon, \qquad (2.10)$$

$$\beta(t,x) = \frac{\sqrt{A}x}{\frac{\sigma^2}{2}\sinh\left(\frac{\sqrt{A}t}{2}\right)}, \qquad (2.11)$$

$$K(t) = \frac{1}{\sigma^2}\left(\sqrt{A}\coth\left(\frac{\sqrt{A}t}{2}\right)+\kappa\right), \qquad (2.12)$$

where Γ and $_1F_1$ denote the Gamma function and the confluent hypergeometric function respectively.

If

$$\gamma < -\frac{\sqrt{\kappa^2+2\epsilon\sigma^2}+\kappa}{\sigma^2}, \qquad (2.13)$$

then the transform is well defined for all $t < t^*$, with

$$t^* = \frac{1}{\sqrt{A}}\log\left(1-\frac{2\sqrt{A}}{\kappa+\sigma^2\gamma+\sqrt{A}}\right). \qquad (2.14)$$

Remark 2.1 Special case: when $\epsilon = \nu = \gamma = 0$, we have the (non-integral) moments of the process for $\eta < \frac{2\kappa\theta}{\sigma^2}$:

$$\mathbb{E}\left[X_t^{-\eta}\right] = \left(\frac{\kappa}{\sigma^2}\right)^\eta \left(\sinh\left(\frac{\kappa t}{2}\right)\right)^{-\frac{2\kappa\theta}{\sigma^2}} \exp\left(\frac{\kappa}{\sigma^2}\left(\kappa\theta t + x - x\coth\left(\frac{\kappa t}{2}\right)\right)\right)$$

$$\times \left(1+\coth\left(\frac{\kappa t}{2}\right)\right)^{\eta-\frac{2\kappa\theta}{\sigma^2}} \frac{\Gamma\left(\frac{2\kappa\theta}{\sigma^2}-\eta\right)}{\Gamma\left(\frac{2\kappa\theta}{\sigma^2}\right)}$$

$$\times_1 F_1\left(\frac{2\kappa\theta}{\sigma^2}-\eta, \frac{2\kappa\theta}{\sigma^2}, \frac{2\kappa x}{\sigma^2(e^{\kappa t}-1)}\right)$$

$$=: G(\kappa,\theta,\sigma,\eta;t,x).$$

Proof of Lemma 2.1 The result immediately follows Theorem 1 in Grasselli (2017) of which the proof mainly relies on Lie's classical symmetry method as in Bluman and Kumei (1989) and Olver (1993). We first note that by standard arguments the expectation is related to the solution of the following symmetrical PDE:

$$u_t = \frac{1}{2}\sigma^2 x u_{xx} + f(x)u_x - \left(\frac{\nu}{x} + \epsilon x\right)u, \quad \epsilon > 0, \ \nu > 0, \qquad (2.15)$$

where $f(x) = \kappa\theta - \kappa x$. To find the Lie groups admitted by the PDE, the key result states that one should find the invariant surface for the second prolongation of group acting on the $(x; t; u)$-space where the solutions of PDE stay. Once such equations are solved, one can find the corresponding Lie group admitted by the PDE as well as a fundamental solution of the PDE by inverting a Laplace transform. Finally, Craddock and Lennox (2009) offered the condition under which the fundamental solution is also a transition probability density for the underlying stochastic process. For more details, refer to Grasselli (2017). □

Following Goard and Mazur (2013), together with mind-alike authors, we apply the same technique to estimate the parameters in the continuous-time model and create hypothesis testing to judge whether these parameters impose unreasonable overidentifying restrictions. What we would like to emphasize is that our estimation is slightly different from Goard and Mazur's work (Goard and Mazur 2013), expect for the conceptual similarities. One of the differences is on data selection. Instead of directly modeling the VIX, our VIX formula in (2.1) and (2.2) is derived from the dynamics of underlying index. Therefore, we use S&P500 rather than VIX data to estimate. From another perspective, we use the latest one-year period S&P500 index data: January 2, 2016–December 2, 2016. In order to testify whether these parameters impose the mentioned unreasonable overidentifying restrictions on each model, we have strategically divided the one-year period into three sub-ones: January 2, 2016 to December 2, 2016; January 2, 2016 to April 2, 2016 (Period A), May 2, 2016 to August 2, 2016 (Period B) and September 2, 2016 to December 2, 2016 (Period C). Each of these four periods is used to test whether our free stochastic volatility parameter α changes significantly with different periods in 2016. According to Appendix for detailed computation process, we rewrite the corresponding discrete-time econometric specification:

$$\frac{S_{t+1} - S_t}{S_t} = r\Delta t + \varepsilon_{t+1}, \qquad (2.16)$$

$$\begin{aligned}
\mathbb{E}^{\mathbb{P}}\left[\varepsilon_{t+1}\right] &= \delta_s^* \cdot \Delta t \cdot G(\kappa^*, \theta^*, \sigma, -1; \Delta t, V_t) \\
&= \delta_s^* \cdot \Delta t \cdot \left[V_t e^{-\kappa^* \Delta t} + \theta^* \left(1 - e^{-\kappa^* \Delta t}\right)\right] \\
&=: \Psi_1(\kappa^*, \theta^*, \delta_s^*, \sigma, \Delta t), \qquad (2.17)
\end{aligned}$$

$$\begin{aligned}
\mathbb{E}^{\mathbb{P}}\left[\varepsilon_{t+1}^2\right] &= \delta_s^{*2} \cdot \Delta t^2 \cdot G(\kappa^*, \theta^*, \sigma, -2; \Delta t, V_t) \\
&\quad + \gamma^{*2} \cdot \Delta t \cdot G(\kappa^*, \theta^*, \sigma, -2\alpha; \Delta t, V_t) \\
&=: \Psi_2(\kappa^*, \theta^*, \gamma^*, \delta_s^*, \alpha, \sigma, \Delta t), \qquad (2.18)
\end{aligned}$$

Our econometric approach is to estimate parameters of this process and tests Eqs. (2.16)–(2.18) as a set of overidentifying restrictions on a system of moment equations using the GMM of Hansen (1982). As stated by Chan et al. (1992), the intrinsic advantages that this method owns make itself an intuitive and logical choice for continuous-time volatility process estimation. Firstly, it makes no assumptions

about the distributional nature of the changes in S&P500. Also the asymptotic justification for the GMM procedure requires only that the distribution changes are stationary and ergodic, and that the relevant expectations exist. At last GMM estimators and their standard errors are consistent even if the disturbances are conditionally heteroskedastic.

Now we denote ω by a parameter vector with elements κ^*, θ^*, σ, γ^*, δ_s^* and α, then let the vector $m_t(\omega)$ be

$$
m_t(\omega) = \begin{bmatrix}
\varepsilon_{t+1} - \Psi_1(\kappa^*, \theta^*, \delta_s^*, \sigma, \Delta t) \\
\left(\varepsilon_{t+1} - \Psi_1(\kappa^*, \theta^*, \delta_s^*, \sigma, \Delta t)\right) S_t \\
\left(\varepsilon_{t+1} - \Psi_1(\kappa^*, \theta^*, \delta_s^*, \sigma, \Delta t)\right) S_t^2 \\
\varepsilon_{t+1}^2 - \Psi_2(\kappa^*, \theta^*, \gamma^*, \delta_s^*, \alpha, \sigma, \Delta t) \\
\left(\varepsilon_{t+1}^2 - \Psi_2(\kappa^*, \theta^*, \gamma^*, \delta_s^*, \alpha, \sigma, \Delta t)\right) S_t \\
\left(\varepsilon_{t+1}^2 - \Psi_2(\kappa^*, \theta^*, \gamma^*, \delta_s^*, \alpha, \sigma, \Delta t)\right) S_t^2
\end{bmatrix}.
\tag{2.19}
$$

Under the null hypothesis that the restrictions implied in Eqs. (2.17)–(2.18) are true, the orthogonality conditions, $\mathbb{E}^{\mathbb{P}}[m_t(\omega)] = 0$, hold. Because we directly use S&P500 market data to estimate paramaters, all expectations should be calculated under the physical probability measure $\mathbb{P}$. The GMM technique replaces $\mathbb{E}^{\mathbb{P}}[m_t(\omega)]$ with its sample counterpart $M_T(\omega)$ using the T observations where $M_T(\omega) = \frac{1}{T} \sum_{t=1}^{T} m_t(\omega)$ and then chooses parameters which minimize the quadratic form

$$
J_T(\omega) = M_T'(\omega) W_T(\omega) M_T(\omega),
\tag{2.20}
$$

where $W_T(\omega)$ is a positive definite symmetric weighting matrix. The GMM estimates of the overidentified parameter subvector of ω do depend on the choice of $W_T(\omega)$. Hansen (1982) provided that by setting $W_T(\omega) = S^{-1}(\omega)$, where $S(\omega) = \mathbb{E}^{\mathbb{P}}[m_t(\omega) m_t'(\omega)]$, it delivers the GMM estimator of ω with the smallest asymptotic covariance matrix. The minimized value of the quadratic form in (2.20) is distributed χ^2 under the null hypothesis that the model is true with degrees of freedom equal to the number of orthogonality conditions net of the number of parameters to be estimated. This χ^2 measure provides a goodness-of-fit test for the model. A hypothesis test is then used to test whether the models impose unreasonable overidentifying restrictions upon the unrestricted model, i.e., for each nested model, we create the hypothesis test of a_0 versus a_1 where

a_0: The model does not impose overidentifying restrictions and is hence not misspecified;

a_1: The model does impose overidentifying restrictions and is hence misspecified.

The test statistic, $R = T\left[J_T(\tilde{\omega}) - J_T(\hat{\omega})\right]$, is asymptotically distributed χ^2 with degrees of freedom equal to the number of restrictions on the general model to obtain the nested model. Specifically, the combination of (2.1) and (2.2) is the general model with six unrestricted parameters so it is called unrestricted model. When $\alpha = \frac{1}{2}$ and $\gamma^* = 1$, for instance, are determined in unrestricted model, a nested model is obtained, namely the famous Heston model. The number of restrictions is equivalent

to the degrees of freedom of χ^2. By using the same weighting matrix from the unrestricted model, this test statistic is the normalized difference of the restricted $J_T(\tilde{\omega})$ and unrestricted $J_T(\hat{\omega})$ objective functions for the efficient GMM estimator. A high value of this statistic indicates that the model is misspecified. Once the p value is below the required level of significance, here we can draw a conclusion that this model is misspecified.

With a view to a full and complete description, the GMM results are presented in Table 1. Parameters of all estimations have small standard deviations, hence they are stable. Firstly, with regard to the reported χ^2 values from the whole period estimation, Heston and 3/2 models are rejected at the 1% level of significance. This fact shall contribute to explaining that the internal working of Heston and 3/2 models fails to match S&P500 data. Therefore, these models are misspecified and given the irrational restrictions on the unrestricted model. On the other hand, FSV model results in acceptance at the 1% level significance with p value of 0.767, since a new parameter α that FSV model contains contributes to S&P500 matching. So the model is not misspecified. Thirdly, we re-estimate the parameters under the free stochastic model with different periods in 2016. Given that free stochastic model having $\alpha = 0.864$ in Period A, $\alpha = 0.901$ in Period B, and $\alpha = 0.943$ in Period C, we would like to draw the conclusion that the volatility fluctuations that α implies vary in periods, and should be taken into consideration in our model. Heuristically, the FSV model with free volatility parameter α matches S&P500 which is widely regarded as frequent fluctuation index. Compared with FSV model's decent matching performance, Heston and 3/2 model are rejected. Through the results from unrestricted model, we find that γ^* shows ignorable influence over results. Thus, $\gamma^* = 1$ is acceptable and reasonable.

3 Free stochastic volatility plus asymmetric jumps model

Sepp (2008) asserted that "stochastic volatility models without jumps are not consistent with the implied volatility skew observed in options on the VIX..." and that "...only the stochastic volatility with appropriately chosen jumps can fit the implied VIX skew". However, the jump sizes modeled in Heston (1993), Baldeaux and Badran (2014), and even Lian and Zhu (2013) are distributed to be normal in underlying dynamics. Normal jump makes upward and downward jumps symmetric due to its central mean and variance. However, it is not uncommon to observe that the equity market often appears to be more volatile on the downside than the upside. Based on this observation, upward and downward jumps in underlying dynamics are respectively assumed, and driven by independent compound Possion processes. We firstly extends free stochastic volatility to the asset-price process with asymmetric jumps. This is a new family of free volatility and jump-diffusion models for VIX dynamics. We derive semi-closed-form solution to the prices of futures and options. In addition, we provide a description for our estimation method, and introduce a competing model from Heston and 3/2 models plus jumps. The Heston model is a limiting case of all other models and viewed as the benchmark in our empirical study. Then, we demonstrate when the underlying asset price process includes FSV parameter α and asymmetric jumps, the VIX formula remains valid.

Table 1 We estimate the parameters for processes of different models nested within Eq. (2.1) with its standard error in parentheses to test the significance of the individual parameters

Model	κ^*	θ^*	σ	γ^*	δ_s^*	α	χ^2	DF
The whole period: January 2, 2016–December 2, 2016								
Unrestricted	1.513	0.475	0.509	1.011	− 0.337	1.274	N/A	N/A
	<[0.001]	<[0.001]	<[0.001]	<[0.012]	<[0.281]	<[0.08]		
Heston	2.829	0.020	0.831	1	−4.394	0.5	16.583	2
	<[0.001]	<[0.001]	<[0.001]		<[2.012]		<[0.001]	
3/2 model	10.29	56.49	− 2.598	1	− 0.016	− 0.5	15.457	2
	<[0.001]	<[0.001]	<[0.03]		<[0.032]		<[0.001]	
Free stochastic	2.036	0.502	0.650	1	− 0.526	1.288	0.087	1
	<[0.001]	<[0.001]	<[0.001]		<[0.259]	<[0.01]	0.767	
Period A: January 2, 2016–April 2, 2016								
Free stochastic	1.699	0.617	0.484	1	− 0.745	0.864	3.866	1
	<[0.001]	<[0.001]	<[0.001]		<[0.022]	<[0.02]	0.0492	
Period B: May 2, 2016–August 2, 2016								
Free stochastic	2.326	0.695	0.687	1	− 0.692	0.901	1.654	1
	<[0.001]	<[0.001]	<[0.001]		<[0.058]	<[0.07]	0.1983	
Period C: September 2, 2016–December 2, 2016								
Free stochastic	1.911	0.387	0.469	1	− 0.821	0.943	1.119	1
	<[0.001]	<[0.001]	<[0.001]		<[0.074]	<[0.05]	0.289	

The χ^2 test statistics are computed following the method outlined in Whitney (1985) with p value in parentheses and associated degrees of freedom (*DF*). GMM method estimates the values of parameters from the historical data over four different periods: The whole Period, Period A, Period B, Period C. Periods A–C are only used in free stochastic model

For option pricing, we follow the standard approach of using the risk-neutral pricing idea, which implies that the discounted asset price process is a martingale with respect to an equivalent martingale measure, $\mathbb{Q}$. The choice of equivalent martingale measure shown as below is consistent with the one in Heston (1993), Bates (2000) and Pan (2002) for the volatility risk premium, in terms of market incompleteness dealing, aroused by stochastic volatility. Consider the dynamics for the underlying index under such measure $\mathbb{Q}$ given by:

$$\frac{dS_t}{S_t} = (r - \lambda_1 \tilde{\mu}_1 - \lambda_2 \tilde{\mu}_2)dt + V_t^\alpha dW_t^{\mathbb{Q}}$$

$$+(e^{J_1^{\mathbb{Q}}} - 1)dN_{1t}^{\mathbb{Q}} + (e^{J_2^{\mathbb{Q}}} - 1)dN_{2t}^{\mathbb{Q}}, \tag{3.1}$$

$$dV_t = \kappa\left(\theta - V_t\right)dt + \sigma\sqrt{V_t}dZ_t^{\mathbb{Q}}, \tag{3.2}$$

where $\kappa = \kappa^* + \delta_v$, $\theta = \frac{\kappa^*\theta^*}{\kappa^*+\delta_v}$, $W_t^{\mathbb{P}} = W_t^{\mathbb{Q}} - \delta_s^* \int_0^t V_s^{1-\alpha}ds$ and $Z_t^{\mathbb{P}} = Z_t^{\mathbb{Q}} - \delta_v/\sigma \int_0^t V_s^{1/2}ds$ with δ_v being interpreted as the volatility risk premium. $W_t^{\mathbb{Q}}$ and $Z_t^{\mathbb{Q}}$ are two correlated Brownian processes under risk-neutral measure $\mathbb{Q}$, and their correlation coefficient remains to be ρ. As for asymmetric jumps, we emphasize again that this jump is conceptually different to Park's work (2016). Instead of directly modeling jumps-added and non-underlying-index VIX, we establish upward and downward in underlying index. To be more specific, we assume that the upward and downward are driven by independent compound Possion processes, each having its own jump intensity and jump-size distribution. $N_{1t}^{\mathbb{Q}}$ and $N_{2t}^{\mathbb{Q}}$ denote risk-neutral Possion processes driving upward and downward jumps with jump intensities λ_1 and λ_2, respectively.

Upward jump magnitudes, $J_1^{\mathbb{Q}}$, are assumed to follow an independent exponential distribution with a positive mean, $\mu_1 > 0$. Its probability density function shall take $\frac{1}{\mu_1}\exp(-x/\mu_1)$ if $x > 0$; for the other situations, it takes 0. The inside parameters $\mu_1, \tilde{\mu}_1$ satisfy the following relationship:

$$\tilde{\mu}_1 = \frac{1}{1-\mu_1} - 1.$$

Under this assumption, $e^{J_1^{\mathbb{Q}}} - 1 > 0$ satisfies upward jump condition. The term $\lambda_1\tilde{\mu}_1 dt$ is used to centralize the Possion innovation so that $(e^{J_1^{\mathbb{Q}}} - 1)dN_{1t}^{\mathbb{Q}} - \lambda_1\tilde{\mu}_1 dt$ has its mean equal to 0. Similarly, downward jump magnitudes, $J_2^{\mathbb{Q}}$, are assumed to follow an independent exponential distribution with a negative mean, $\mu_2 < 0$. Its probability density function takes $\frac{1}{|\mu_2|}\exp(-x/\mu_2)$ if $x < 0$; for the other situations, it takes 0. The inside parameters $\mu_2, \tilde{\mu}_2$ satisfy the following relationship:

$$\tilde{\mu}_2 = \frac{1}{1-\mu_2} - 1.$$

Under this assumption, $-1 < e^{J_2^{\mathbb{Q}}} - 1 < 0$ reaches downward jump condition. The term $\lambda_2\tilde{\mu}_2 dt$ is used to centralize the Possion innovation so that $(e^{J_2^{\mathbb{Q}}} - 1)dN_{2t}^{\mathbb{Q}} - \lambda_2\tilde{\mu}_2 dt$ has its mean equal to 0.

Integrating (3.1) yields

$$S_t = \tilde{S}_t \prod_{s=1}^{N_{1t}} e^{J_{1s}^{\mathbb{Q}}} \prod_{s=1}^{N_{2t}} e^{J_{2s}^{\mathbb{Q}}}, \tag{3.3}$$

where

$$\tilde{S}_t = S_0 \exp\left\{ \int_0^t \left(r - \lambda_1 \tilde{\mu}_1 - \lambda_2 \tilde{\mu}_2 - \frac{1}{2} V_s^{2\alpha} \right) ds + \int_0^t V_s^{\alpha} dW_s^{\mathbb{Q}} \right\},$$

and $J_{1s}^{\mathbb{Q}}$ and $J_{2s}^{\mathbb{Q}}$ denote the respective logarithm of jump size of sth jump, both positive and negative. Because the model in Eqs. (3.1) and (3.2) is not affine, Eq. (3.3) provides us an important starting point for analysis. In particular, one can determine that the discounted stock price is a true martingale rather than a local one under our assumed model.

Proposition 3.1 *Let S and V be given by Eqs.* (3.1) *and* (3.2) *respectively. Then the discounted stock price* $\bar{S}_t = \frac{S_t}{e^{rt}}$ *is a true martingale, and not just a strict local martingale under* $\mathbb{Q}$.

Proof We assume that the discounted stock price is $\bar{S}_t = \frac{S_t}{e^{rt}}$ and compute

$$\mathbb{E}^{\mathbb{Q}}\left[\bar{S}_T | \mathscr{F}_t \right] = \mathbb{E}_t^{\mathbb{Q}}\left[\frac{\tilde{S}_T \prod_{s=1}^{N_{1T}} e^{J_{1s}^{\mathbb{Q}}} \prod_{s=1}^{N_{2T}} e^{J_{2s}^{\mathbb{Q}}}}{e^{rT}} \right]$$

$$= \mathbb{E}_t^{\mathbb{Q}}\left[\frac{\tilde{S}_t \prod_{s=1}^{N_{1T}} e^{J_{1s}^{\mathbb{Q}}} \prod_{s=1}^{N_{2T}} e^{J_{2s}^{\mathbb{Q}}}}{e^{rt}} \cdot \frac{\exp\left\{ \int_t^T \left(r - \lambda_1 \tilde{\mu}_1 - \lambda_2 \tilde{\mu}_2 - \frac{1}{2} V_s^{2\alpha} \right) ds + \int_t^T V_s^{\alpha} dW_s^{\mathbb{Q}} \right\}}{e^{r(T-t)}} \right]$$

$$= \bar{S}_t \cdot \mathbb{E}_t^{\mathbb{Q}}\left[\exp\left\{ \int_t^T \left(-\lambda_1 \tilde{\mu}_1 - \lambda_2 \tilde{\mu}_2 - \frac{1}{2} V_s^{2\alpha} \right) ds + \int_t^T V_s^{\alpha} dW_s^{\mathbb{Q}} \right\} \right.$$

$$\times \left. \prod_{s=N_t+1}^{N_{1T}} e^{J_{1s}^{\mathbb{Q}}} \prod_{s=N_t+1}^{N_{2T}} e^{J_{2s}^{\mathbb{Q}}} \right]$$

$$= \bar{S}_t \cdot \mathbb{E}_t^{\mathbb{Q}}\left[\exp\left\{ \int_t^T \left(-\lambda_1 \tilde{\mu}_1 - \lambda_2 \tilde{\mu}_2 - \frac{1}{2} V_s^{2\alpha} \right) ds \right.\right.$$

$$\left.\left. + \int_t^T V_s^{\alpha} dW_s^{\mathbb{Q}} \right\} \right] e^{\lambda_1 (T-t)\tilde{\mu}_1 + \lambda_2 (T-t)\tilde{\mu}_2}$$

$$= \bar{S}_t \cdot \mathbb{E}_t^{\mathbb{Q}}\left[-\frac{1}{2} \int_t^T V_s^{2\alpha} ds \right.$$

$$\left. + \int_t^T V_s^{\alpha} dW_s^{\mathbb{Q}} \right]$$

$$= \bar{S}_t \cdot \mathbb{E}_t^{\mathbb{Q}}\left[-\frac{\rho^2}{2} \int_t^T V_s^{2\alpha} ds + \rho \int_t^T V_s^{\alpha} dZ_s^{\mathbb{Q}} \right]$$

$$= \bar{S}_t \cdot \mathbb{E}_t^{\mathbb{Q}}\left[\xi_{t,T} \right], \tag{3.4}$$

where we define the process $\xi = \{\xi_t, t \geq 0\}$ via

$$\xi_t := \exp\left\{-\frac{\rho^2}{2}\int_0^t V_s^{2\alpha}ds + \rho\int_0^t V_s^\alpha dZ_s^{\mathbb{Q}}\right\}.$$

Apparently, it is an exponential local martingale. In order to judge whether the process $\bar{S}_t = \frac{S_t}{e^{rt}}$ is a martingale, we follow Lewis (2000, Theorem 9.2). Accordingly, the Feller non-explosion test applying over both V_t and its auxiliary volatility process must be satisfied simultaneously. Firstly, under the risk neutral probability measure $\mathbb{Q}$, the process V_t can neither explode to ∞ nor reach to 0 when Feller condition is satisfied, i.e.,

$$2\kappa\theta \geq \sigma^2.$$

Additionally, Feller non-explosion test involves transformation of $\mathbb{Q}$ to the auxiliary process $\hat{\mathbb{Q}}$, but without the corresponding change in viewpoint to use shares as numeraire:

$$dZ_t^{\hat{\mathbb{Q}}} = dZ_t^{\mathbb{Q}} - \rho V_t^\alpha dt.$$

Under this measure, the auxiliary volatility process V_t solves

$$dV_t = \left(\kappa\theta - \kappa V_t + \sigma\rho V_t^{\alpha+\frac{1}{2}}\right)dt + \sigma\sqrt{V_t}dZ_t^{\hat{\mathbb{Q}}}.$$

We apply the Feller non-explosion test illustrated early in Sect. 3 of Lewis (2000). The scale density is

$$s(V) = V^{-\frac{2\kappa\theta}{\sigma^2}}e^{\frac{2\kappa}{\sigma^2}V - \frac{2\rho}{\sigma}\frac{1}{\alpha+\frac{1}{2}}V^{\alpha+\frac{1}{2}}}.$$

As a consequence the scale measure is given by

$$S(c,d) = \int_c^d s(V)dV = \int_c^d V^{-\frac{2\kappa\theta}{\sigma^2}}e^{\frac{2\kappa}{\sigma^2}V - \frac{2\rho}{\sigma}\frac{1}{\alpha+\frac{1}{2}}V^{\alpha+\frac{1}{2}}}dV \quad \text{for} \ \ 0 < c < d.$$

Assuming $\rho < 0$, then $S(c, +\infty) = \infty$ if and only if $\alpha + \frac{1}{2} > 0$. Since $\alpha \in [-\frac{1}{2}, \frac{3}{2}]$ is required in our model, the divergence result follows. For the speed density, we have

$$m(V) = \frac{1}{\sigma^2 V s(V)} = \frac{1}{\sigma^2}V^{\frac{2\kappa\theta}{\sigma^2}-1}e^{-\frac{2\kappa}{\sigma^2}V + \frac{2\rho}{\sigma}\frac{1}{\alpha+\frac{1}{2}}V^{\alpha+\frac{1}{2}}}.$$

Clearly, $N(\infty) = \lim_{d\uparrow\infty}\int_c^d S(c, x)m(x)dx$ diverges as $d \to \infty$. According to boundary classification criteria, it shows that $S(c, +\infty) = \infty$ and $N(\infty) = \infty$ suffice to classify

$V = \infty$ as an natural boundary under a negative correlation coefficient, which means that there is no explosion in this case, since the boundary is unreachable in finite time. Referring to the collection of our results, the process $\bar{S}_t$ is a martingale. $\qquad \square$

4 Pricing of VIX options and futures

In this section, we derive a general pricing formula for European call options and futures on the VIX of which the index follows FSV process. Firstly, the log contract can be synthesized with a portfolio of call and put options in a continuum of strikes (Breeden and Litzenberger 1978), which leads to the VIX formula (CBOE 2003). Thus, VIX square can be expressed, in terms of the risk-neutral expectation of the log contract. Different dynamics for the index price S_t will result in various expressions for VIX square. Hence, the square VIX index is an approximation to the value of log contract:

$$\text{VIX}_t^2 \approx -\frac{2}{\tau}\mathbb{E}^{\mathbb{Q}}\left[\log\left(\frac{S_{t+\tau}}{S_t e^{r\tau}}\right)\bigg|\mathcal{F}_t\right] \times 100^2, \qquad (4.1)$$

with $\tau = \frac{30}{365}$ and $S_t e^{r\tau}$ being forward price of S&P500 observed at time t with $t + \tau$ as maturity. The VIX formula involves two approximation errors:

(1) when the price dynamics include jumps;
(2) when options are only available for a finite number of strikes.

In the following subsections, we briefly go though Heston and 3/2 models, and present the VIX derivatives pricing formulas in FSV model. The VIX derivatives pricing formula in the following Theorem 4.1 extends both Proposition 3.4 in Baldeaux and Badran (2014), joint with the Proposition 1 in Zhang and Zhu (2006).

4.1 Heston stochastic volatility (HSV)

Setting $\alpha = \frac{1}{2}$ and $\lambda_1 = \lambda_2 = 0$ in Eq. (3.1), we obtain the Heston model. The Heston model, which was first proposed by Heston (1993), has been extensively used and studied, due to its tractability. In specification of HSV, Lian and Zhu (2013) showed that the expectation in Eq. (4.1) can be computed explicitly: $\text{VIX}_t^2 = 100^2 \times (aV_t + b)$ where $a = \frac{1-e^{\kappa\tau}}{\kappa\tau}$ and $b = \theta\left(1 - \frac{1-e^{\kappa\tau}}{\kappa\tau}\right)$. With the transitional probability density function (TPDF) $f_{V_T|V_t}^{\mathbb{Q}}(y)$ of CIR process, inversion of $\text{VIX}_t^2 = 100^2 \times (aV_t + b)$ gives us the TPDF of the VIX index

$$f_{\text{VIX}_T|\text{VIX}_t}^{\mathbb{Q}}(z) = \frac{2z}{100^2 a} \cdot f_{V_T|V_t}^{\mathbb{Q}}\left(\frac{\frac{z^2}{100^2} - b}{a}\right)\mathbb{1}_{\left\{z \geq 100\sqrt{b}\right\}}.$$

Hence, the price of an European call option could be obtained by computing the expected payoff directly as:

$$C\,(\mathrm{VIX}_t, K, t, T) = e^{-r(T-t)} \int_K^\infty \max{(y-K, 0)}\, f^{\mathbb{Q}}_{\mathrm{VIX}_T|\mathrm{VIX}_t}(y) dy, \qquad (4.2)$$

while the VIX futures are:

$$F\,(\mathrm{VIX}_t, t, T) = \mathbb{E}^{\mathbb{Q}}\,[\mathrm{VIX}_T|\mathcal{F}_t] = \int_0^\infty y \cdot f^{\mathbb{Q}}_{\mathrm{VIX}_T|\mathrm{VIX}_t}(y) dy. \qquad (4.3)$$

4.2 3/2 stochastic volatility with jumps in price (3/2-SVJ)

The Heston model struggles to incorporate the smile in the implied volatilities of short-term index options. Baldeaux and Badran showed that unlike 3/2 model, the implied volatilities are downward sloping, which is not consistent with market data. They ended in finding that 3/2 plus jumps model is able to better fit short-term index implied volatilities while produce more realistic VIX option implied volatilities without tractable loss. Setting the volatility parameter $\alpha = -\frac{1}{2}$ in Eq. (3.1), one could arrive at 3/2 plus jump model in Eq. (3.1). After some computation processes, the expectation in Eq. (4.1) can be computed as

$$\mathrm{VIX}_t^2 = \left(\frac{1}{\tau}\mathbb{E}^{\mathbb{Q}}\left[\int_t^{t+\tau} V_t^{-1} dt\right] + 2\left(\lambda_1\left(\tilde{\mu}_1 - \mu_1\right) + \lambda_2\left(\tilde{\mu}_2 - \mu_2\right)\right)\right) \times 100^2$$

$$= \left(\frac{1}{\tau}\int_0^\tau G(\kappa, \theta, \sigma, 1; u, x) du + G_0(\mu_1, \mu_2, \tilde{\mu}_1, \tilde{\mu}_2, \lambda_1, \lambda_2)\right) \times 100^2,$$

for $t \geq 0$. Hence, the price of a European call option in 3/2 stochastic volatility with jumps could be obtained by computing the expected payoff directly as:

$$C\,(\mathrm{VIX}_t, K, t, T) = e^{-r(T-t)}\mathbb{E}^{\mathbb{Q}}\left[(\mathrm{VIX}_T - K)^+|\mathcal{F}_t\right]$$

$$= e^{-r(T-t)} \int_0^\infty \left(100\sqrt{\left(\frac{1}{\tau}\int_0^\tau G du + G_0\right)} - K\right)^+$$

$$\times f^{\mathbb{Q}}_{V_T|V_t}(y) dy, \qquad (4.4)$$

while the VIX futures are:

$$F\,(\mathrm{VIX}_t, K, t, T) = e^{-r(T-t)}\mathbb{E}^{\mathbb{Q}}\,[\mathrm{VIX}_T|\mathcal{F}_t]$$

$$= e^{-r(T-t)} \int_0^\infty \left(100\sqrt{\left(\frac{1}{\tau}\int_0^\tau G du + G_0\right)}\right) f^{\mathbb{Q}}_{V_T|V_t}(y) dy. \qquad (4.5)$$

4.3 Free stochastic volatility and jumps in price (FSV-type)

To capture the free behavior of volatility, we free the power parameter of instantaneous variance, instead of fixing α to be $\frac{1}{2}$ or $-\frac{1}{2}$. We do not restrict the sign of α, allowing data voice its authentic direction.

Theorem 4.1 *Let S, V, and* VIX^2 *be defined by Eqs.* (3.1), (3.2) *and* (4.1). *Then*

$$\mathrm{VIX}_t^2 = 100^2 \times \left(H_1 + \int_0^\tau H_2 du \right), \tag{4.6}$$

where

$$H_1(\lambda_1, \mu_1, \lambda_2, \mu_2) = 2 \left[\lambda_1 \left(\tilde{\mu}_1 - \mu_1 \right) + \lambda_2 \left(\tilde{\mu}_2 - \mu_2 \right) \right], \tag{4.7}$$

$$
\begin{aligned}
H_2(\kappa, \theta, \sigma, \alpha; u, x) = {}& \frac{\sigma^{4\alpha}}{\tau \kappa^{2\alpha}} \frac{\Gamma\left(\frac{2\kappa\theta}{\sigma^2} + 2\alpha \right)}{\Gamma\left(\frac{2\kappa\theta}{\sigma^2} \right)} \left(\sinh\left(\frac{ku}{2} \right) \right)^{-\frac{2\kappa\theta}{\sigma^2}} \\
& \times \exp\left(\frac{\kappa}{\sigma^2} \left(\kappa\theta u + x - x \coth\left(\frac{ku}{2} \right) \right) \right) \\
& \times \left(1 + \coth\left(\frac{ku}{2} \right) \right)^{-2\alpha - \frac{2\kappa\theta}{\sigma^2}} {}_1F_1 \left(\frac{2\kappa\theta}{\sigma^2} \right. \\
& \left. + 2\alpha, \frac{2\kappa\theta}{\sigma^2}, \frac{2\kappa x}{\sigma^2(e^{\kappa u} - 1)} \right).
\end{aligned}
\tag{4.8}
$$

Proof From Eqs. (3.3) and (4.1), we get

$$
\begin{aligned}
\frac{\mathrm{VIX}_t^2}{100^2} = {}& -\frac{2}{\tau} \mathbb{E}^{\mathbb{Q}} \left[(-\lambda_1 \tilde{\mu}_1 - \lambda_2 \tilde{\mu}_2) \tau - \frac{1}{2} \int_t^{t+\tau} V_s^{2\alpha} ds + \sum_{i=N_1(t)+1}^{N_1(t+\tau)} J_{1i}^{\mathbb{Q}} \right. \\
& \left. + \sum_{i=N_2(t)+1}^{N_2(t+\tau)} J_{2i}^{\mathbb{Q}} \middle| \mathcal{F}_t \right] \\
= {}& 2 (\lambda_1 \tilde{\mu}_1 + \lambda_2 \tilde{\mu}_2) + \frac{1}{\tau} \int_t^{t+\tau} \mathbb{E}^{\mathbb{Q}} \left[V_s^{2\alpha} | \mathcal{F}_t \right] ds \\
& - \frac{2}{\tau} \mathbb{E}^{\mathbb{Q}} \left[\sum_{i=N_1(t)+1}^{N_1(t+\tau)} J_{1i}^{\mathbb{Q}} + \sum_{i=N_2(t)+1}^{N_2(t+\tau)} J_{2i}^{\mathbb{Q}} \middle| \mathcal{F}_t \right] \\
= {}& 2 \left[\lambda_1 \left(\tilde{\mu}_1 - \mu_1 \right) + \lambda_2 \left(\tilde{\mu}_2 - \mu_2 \right) \right] + \frac{1}{\tau} \int_0^\tau \mathbb{E}^{\mathbb{Q}} \left[V_s^{2\alpha} | \mathcal{F}_t \right] ds \\
= {}& 2 \left[\lambda_1 \left(\tilde{\mu}_1 - \mu_1 \right) + \lambda_2 \left(\tilde{\mu}_2 - \mu_2 \right) \right] \\
& + \int_0^\tau \frac{\sigma^{4\alpha}}{\tau \kappa^{2\alpha}} \frac{\Gamma\left(\frac{2\kappa\theta}{\sigma^2} + 2\alpha \right)}{\Gamma\left(\frac{2\kappa\theta}{\sigma^2} \right)} \left(\sinh\left(\frac{ku}{2} \right) \right)^{-\frac{2\kappa\theta}{\sigma^2}}
\end{aligned}
$$

$$\times \exp\left(\frac{\kappa}{\sigma^2}\left(\kappa\theta u + x - x \coth\left(\frac{\kappa u}{2}\right)\right)\right)$$

$$\times \left(1 + \coth\left(\frac{\kappa u}{2}\right)\right)^{-2\alpha - \frac{2\kappa\theta}{\sigma^2}} {}_1F_1\left(\frac{2\kappa\theta}{\sigma^2} + 2\alpha, \frac{2\kappa\theta}{\sigma^2}, \frac{2\kappa x}{\sigma^2(e^{\kappa u} - 1)}\right) ds$$

$$= H_1(\lambda_1, \mu_1, \lambda_2, \mu_2) + \int_0^\tau H_2(\kappa, \theta, \sigma, \alpha; u, x) du. \tag{4.9}$$

Here we used Remark 2.1 to set $\eta = 2\alpha$, and noticed that V_t is a Markov process. ☐

It should be noted that Eq. (4.9) is useful as it shows that the distribution of VIX_t^2 can be obtained via the distribution of V_t, for $t \geq 0$. That is to say, the problem of pricing VIX derivatives is equivalent to the problem of finding the transition density function for the variance process. By using Eq. (3.3), the price of a European call option in free stochastic volatility model can be obtained by computing the expected payoff directly as:

$$C\,(\text{VIX}_t, K, t, T) = e^{-r(T-t)} \mathbb{E}^{\mathbb{Q}}\left[(\text{VIX}_T - K)^+ | \mathcal{F}_t\right]$$

$$= e^{-r(T-t)} \int_0^\infty \left(100\sqrt{H_1 + \int_0^\tau H_2 du} - K\right)^+ \cdot f_{V_T|V_t}^Q(y) dy, \tag{4.10}$$

while the VIX futures are:

$$F\,(\text{VIX}_t, K, t, T) = e^{-r(T-t)} \mathbb{E}^{\mathbb{Q}}\left[\text{VIX}_T | \mathcal{F}_t\right]$$

$$= e^{-r(T-t)} \int_0^\infty 100\sqrt{H_1 + \int_0^\tau H_2 du} \cdot f_{V_T|V_t}^Q(y) dy. \tag{4.11}$$

Four stochastic volatility models can be nested within the Eqs. (3.1) and (3.2). We select different specifications in accordance with the restrictions on α, λ_1, or λ_2. The model specifications considered in this paper are summarized in Table 2.

Table 2 Summary of model specifications

Model	Description	Constraints
HSV	Fixed volatility, no jumps	$\alpha = \frac{1}{2}$, $\lambda_1 = 0$, and $\lambda_2 = 0$
3/2-SVJ	Fixed volatility, upward and downward jumps	$\alpha = -\frac{1}{2}$
FSV-AJ	Free volatility, upward and downward jumps	N/A
FSV-DJ	Free volatility, downward jumps only	$\lambda_1 = 0$

(a)

(b)
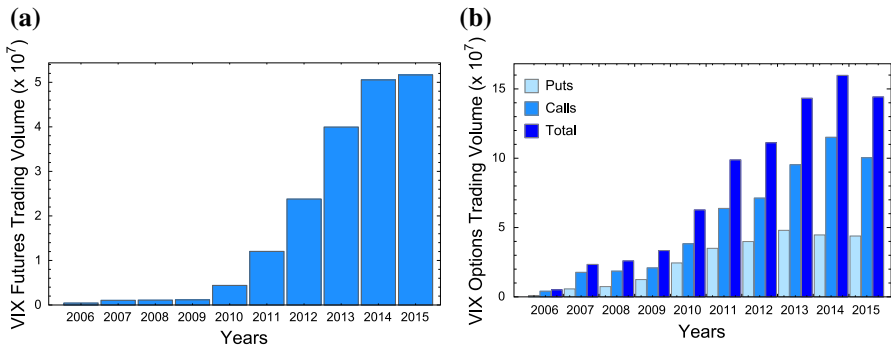
Fig. 2 Trading volume of VIX futures and options. The left panel shows the numbers of futures contracts traded over time, while the right panel presents the dollar trading volumes for options contracts over time. **a** Futures Trading Volume, **b** Options Trading Volume

5 Data description

Our application eyes at the valuation of VIX futures and options, among other volatility derivatives. The market for those derivatives has witnessed explosive growth in trading activity in recent years (see Fig. 2). The left panel of Fig. 2 shows that the number of VIX future contract increases dramatically from about 0.4 million in 2006 to about 51 million in 2015, and most of the growth occurs after 2009, perhaps provoked by the financial crisis. Figure 2a also indicates that VIX futures reflect a demand for tradable vehicle which can be used to hedge or implement a view on volatility. The right panel of Fig. 2 presents that the dollar trading volume for the VIX options increases substantially from around 5 million in 2006 to nearly 150 million in 2015. Note that VIX call options are more actively traded than VIX put option, which may be associated with the fact that the former, unlike the latter, can be used as a means of hedging a stock market crash.

Our data set used in this work comprises VIX index, the corresponding VIX futures and options traded on the CBOE, fully considering that the option written on this index is one of the most actively traded contracts. We endeavor to contain the dates on which both VIX futures and options are available. Under this framework, the future sample contains 193 futures with a total of 23 trading days and available maturities from 1 day to 268 days, while the option sample contains 872 call options with a total of 10 trading days and available maturities from 1 day to 169 days. Furthermore, our in-sample data employs the delayed market quotes over the period starts on March 1, 2016, and ends on March 20, 2016, with 9 to 10 maturities for each trading day, to calibrate the risk-neutral parameters.

Besides, we use those from March 21, 2016 to March 31, 2016 for the out-of-sample test. All details are shown in Table 3. In this table, we also categorize the data depending on time to maturity τ and relevant moneyness $d = \text{VIX}/K$, where K is the strike. Time to maturity τ contains short-term contracts with $\tau \le$ one month, middle-term contracts with one month $< \tau \le$ three months, and long-term contracts with $\tau >$ three months. Their moneyness d is divided into three categories: Out-of-The-Money

Table 3 Summary statistics for overall sample

		Time to maturities			
		Short	Middle	Long	Total
All futures	No. of futures	21	43	129	193
	Average price	17.47	19.23	20.95	20.18
All options	No. of options	314	222	336	872
	Average price	5.85	5.41	4.41	5.18
OTM options	No. of options	9	61	219	289
$(d < -0.1)$	Average price	2.50	2.81	3.16	3.07
	Average BSIV	0.79	0.72	0.65	0.67
ATM options	No. of options	51	48	64	163
$(-0.1 \leq d \leq 0.1)$	Average price	3.45	4.53	5.41	4.54
	Average BSIV	0.73	0.57	0.53	0.61
ITM options	No. of options	254	113	53	420
$(0.1 < d)$	Average price	6.45	7.19	8.34	6.89
	Average BSIV	0.87	0.57	0.46	0.73

Detail descriptions of VIX option	Total	Moneyness $d = \text{VIX}/K$		
		OTM ≤ -0.1	ATM $(-0.1, 0.1)$	ITM ≥ 0.1
Mar. 1–Mar. 20, 2016	$5.17	$2.98	$4.11	$6.77
	(669)	(199)	(119)	(351)
Mar. 21–Mar. 31, 2016	$5.24	$3.27	$5.71	$7.53
	(203)	(90)	(44)	(69)

The moneyness is defined as $d = \text{VIX}/K$, where K is the strike of option. Short-term contracts are those with no more than one month to maturity, middle-term contracts are those between one and three months to maturity, and long-term contracts are those more than three months to maturities. Detailed descriptions of VIX option data show that the reported numbers are respectively the average option price and the numbers of observations, which are shown in the parenthesis, for the overall sample and each moneyness category from March 1, 2016 to March 31, 2016. BSIV stands for Black-Scholes implied volatility. OTM, ATM, ITM denote Out-of-the-Money, At-the-Money, In-the-Money options, respectively

(OTM) with $d < -0.1$, At-The-Money (ATM) with $-0.1 \leq d \leq 0.1$ and In-The-Money (ITM) with $0.1 < d$. For each category, we describe the corresponding sample size, average price and average implied volatility. Finally, we calculate Black-Scholes implied volatility when options are in ITM, ATM and OTM. Option prices are taken from the bid-ask midpoint. To ensure sufficient liquidity and alleviate the influence of price discreetness during the valuation, a filtering scheme is applied to eliminate inaccurate options by discarding options of which the mid price is less than $2.0 in all data set. Note that the closing hour is same for both options and VIX, thus there is no non-synchronous issue. Finally, the average one-month US Treasury Bond Rate, 0.05% is chosen to be the risk free interest rate in the period from March 1, 2016 to March 31, 2016.

6 Parameter estimates and methodology

6.1 Estimation methodology

The estimation procedure begins by separately minimizing the "loss function" according to model genre and given day, so as to derive the risk neutral parameters. As the VIX index and VIX options both contain information concerning the future dynamics of VIX index, the following loss functions contain VIX index and VIX options, respectively:

$$\text{VIX}Loss = \frac{1}{N_1} \sum_{n=1}^{N_1} \frac{\left| \text{VIX}_n - \widehat{\text{VIX}}_n \right|}{\text{VIX}_n},$$

and

$$OptionLoss = \frac{1}{N_2} \sum_{n=1}^{N_2} \frac{\left| C_n - \widehat{C}_n \right|}{C_n},$$

where N_i $(i = 1, 2)$ is the number of sample data, then $\text{VIX}_n, \widehat{\text{VIX}}_n, C_n$ and $\widehat{C}_n$ respectively represent the market VIX index, model VIX index, the market option price and model option price. In this section, we adopt a gradient-based minimization algorithm as well as a local optimization scheme to minimize the two loss functions. Note, the minimization of loss functions is a non-linear optimization problem, which might lead to different optimal parameters for various starting parameters. Therefore, the success of scheme depends on effective choices of the initial parameters. To address this problem, we at first minimize the $\text{VIX}Loss$ function by running calibration 40 times with reasonable parameters chosen from the previous literature or GMM estimation. Then, we record a set of VIX-optimum parameters as initial values. Next, we use those VIX-optimum parameters as initial parameters and search for new estimates by minimizing $OptionLoss$ function. Throughout all calibrations, the Feller's condition $\frac{2\kappa^*\theta^*}{\sigma^2} > 1$ and non-explosion condition $\frac{2\kappa^*\theta^*}{\sigma^2} > 1 - \alpha$ are imposed. In fact, these two conditions are equivalent to $\frac{2\kappa\theta}{\sigma^2} > 1$ and $\frac{2\kappa\theta}{\sigma^2} > 1 - \alpha$ due to $\kappa\theta = \kappa^*\theta^*$ which can be calculated from $\kappa = \kappa^* + \delta_v$ and $\theta = \frac{\kappa^*\theta^*}{\kappa^* + \delta_v}$. In addition, we impose additional calculation on updating Hessian matrix approximation at each iteration by using BFGS formula in quasi-Newton method. Hence, standard deviation of each parameter can be computed through inverse of Hessian matrix in each iteration. In the final stage, we examine whether FSV and jumps would help to match the observed term structure of implied volatility; in average, which gives us a hint to the pricing performance results discussed in the following section.

6.2 Parameter estimates and preliminary analysis

Table 4 shows that parameters of all models have small standard deviation, hence they are stable. Taking a closer look at the estimates, the FSV models yield very different

Table 4 Estimated of Risk-Neutral Parameters

Parameters	FSV-AJ	FSV-DJ	3/2-SVJ	HSV
κ	3.8943	3.7029	2.4614	3.1490
	(0.010)	(0.010)	(0.009)	(0.003)
θ	0.2121	0.2036	47.313	0.0372
	(0.041)	(0.039)	(0.721)	(0.014)
σ	0.9115	0.8662	-11.0750	1.0880
	(0.016)	(0.012)	(0.118)	(0.031)
α	1.2156	1.1575		
	(0.143)	(0.116)		
λ_1	0.0574		0.0722	
	(0.037)		(0.002)	
μ_1	0.1125		0.1518	
	(0.024)		(0.032)	
λ_2	0.0648	0.0668	0.1203	
	(0.022)	(0.030)	(0.026)	
μ_2	-0.1232	-0.1233	-0.1896	
	(0.021)	(0.001)	(0.141)	
VIX$Loss$	10.20	10.11	10.81	10.32
$OptionLoss$	6.81	7.21	10.65	15.07

Parameters are obtained by minimizing the loss functions over the period March 1, 2016 to March 20, 2016, followed by its standard deviation in parenthesis.. The last two rows, labeled VIX$Loss$ and $OptionLoss$, show the mean absolute percentage errors of VIX (VIX$Loss$), together with the mean absolute percentage errors for all options ($OptionLoss$). Those VIX$Loss$ and $OptionLoss$ are reported in percentages

volatility dynamics in contrast to the non-FSV ones. Given estimation results, we would like to draw some conclusions. Firstly, the last two rows of Table 4 record VIX$Loss$ and $OptionLoss$ of four models, which can be regarded as a comparison metric. We have observed that VIX$Loss$ and $OptionLoss$ in FSV-type models are far lower than other models, which means that FSV models can be more flexible to fit market volatility changes. To be more specific, the gradient-based minimization algorithm is used to minimize the objective function VIX$Loss$ and $OptionLoss$ by running sufficiently many iterations until the objective functions reach the bottom line. The lower values that VIX$Loss$ and $OptionLoss$ appear, the better capability of fitting market VIX index and options they imply. Both information criteria offer decisive rankings of the models: FSV-AJ > FSV-DJ > 3/2-SVJ > HSV (The abbreviations could be referred to Table 2). It can be concluded that free stochastic parameter α presents considerable advantages in pricing VIX derivatives.

Secondly, the FSV-type models ($0.8662 \leq \sigma_{\text{FSV}} \leq 0.9115$) have lower volatility of volatility than the HSV and 3/2-SVJ ($\sigma_{\text{HSV}} = 1.0880$, $\sigma_{3/2\text{-SVJ}} = 11.0750$), hence they are more steady. Thirdly, the jump-related parameters ($\lambda_1, \mu_1, \lambda_2, \mu_2$) in FSV-type play a significant role, suggesting that the underlying asset cannot reject the jump component. When it comes to respective setting, we shall focus on jumps. Table 4 contains the frequencies and sizes of upward and downward jumps in the FSV-AJ and FSV-DJ models. Downward jumps take place about 0.065 times per day with an average size of about 0.123, regardless of the existence of upward jumps. It can be seen that in FSV-AJ model, downward jumps have a higher occurrence rate and a larger
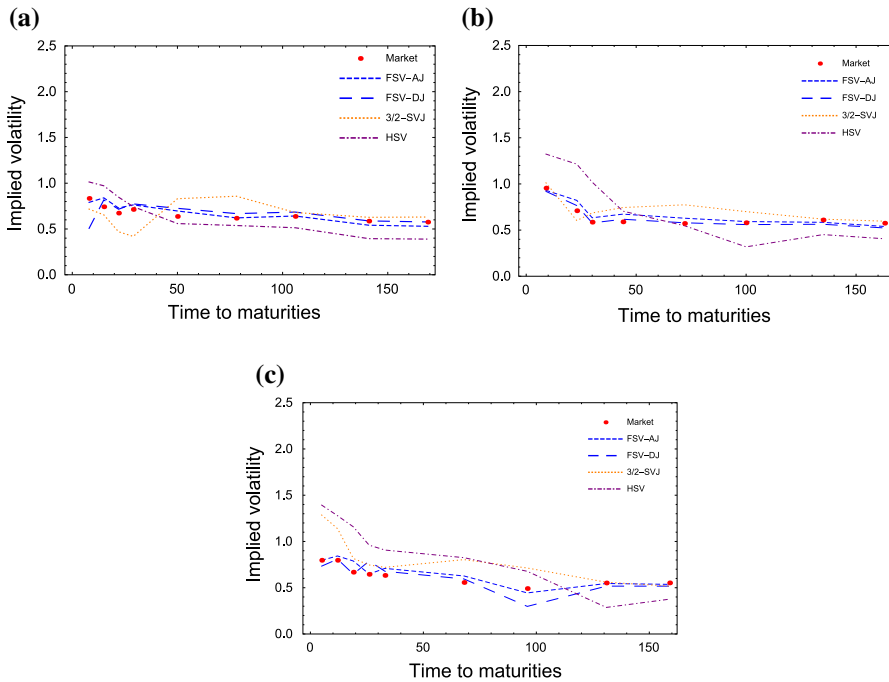
Fig. 3 Graph of VIX's ATM options implied volatility with different maturities. Implied volatilities on March 1, 2016, March 7, 2016 and March 11, 2016 are computed using the market prices and the model-determined prices as inputs to the inverse Black-Scholes formula to obtain the MarketIV and corresponding ModelIV. Only three days are chosen to present. **a** 3/1/2016, **b** 3/7/2016, **c** 3/11/2016

size than upward jumps, namely, $\lambda_2 > \lambda_1$ and $|\mu_2| > \mu_1$. This result also implies that upward and downward jumps should not be normally distributed together. Overall, acceptance for free stochastic parameter α and jumps with respective setting makes a large difference in the estimation of the volatility dynamics of the VIX, which returns a major influenc on the pricing of VIX derivatives.

To earn a capability sense how each model captures the decreasing pattern features in implied volatility, we back out the implied-volatility of each model series from the Black-Scholes formula by taking the model-determined prices as input. Then, we respectively plot the series of the ATM call options with different maturities as reflected in Fig. 3. The three panels in Fig. 3 show that all of the four models—HSV, 3/2-SVJ, FSV-DJ, and FSV-AJ—perform decently in capturing the decreasing pattern in the observed implied volatility. The FSV-type's implied volatility pattern best fits the market skew across different maturities, while HSV and 3/2-SVJ pale in comparison.

7 Pricing performance

Our performance analysis concentrates on three main comparisons. Firstly, we compare the FSV-type models with other models to test the benefits of embracing inside

free stochastic volatility. Secondly, we compare the HSV model with others models to investigate whether the introduction of jumps can make an incremental improvement. Thirdly, we compare FSV-AJ model and FSV-DJ model in order to examine the effects of upward jumps in the case that free stochastic volatility and downward jumps are included.

To facilitate our analysis, we compare the models by reporting the following three measures of performance:

(1) the average relative pricing error (ARPE);
(2) the average relative bid-ask error (ARBAE);
(3) the mean absolute error (MAE):

$$\text{ARPE} = \frac{1}{N} \sum_{i=1}^{N} \frac{\left| Q_i^{Mid} - Q_i^{Model} \right|}{Q_i^{Mid}}, \tag{7.1}$$

$$\text{MAE} = \frac{1}{N} \sum_{i=1}^{N} \left| Q_i^{Model} - Q_i^{Mid} \right|, \tag{7.2}$$

$$\text{ARBAE} = \frac{1}{N} \sum_{i=1}^{N} \frac{\max \left\{ (Q_i^{Model} - Q_i^{Ask})^+, (Q_i^{Bid} - Q_i^{Model})^+ \right\}}{Q_i^{Mid}}. \tag{7.3}$$

The ARPE reports the average pricing error in per cent, while the ARBAE measures the average error of model prices that fall outside the bid-ask spread. MAE stands for the sample average absolute difference between the market price and the model price. We only compute the ARBAE measure for the options, as we do not have available data on bid and ask prices for futures. It should be noted here that Q_i is used to denote quotes on calls and futures.

Table 5 presents in-sample pricing performance across different models. From left to right, the groups of columns show the pricing errors as respectively measured by ARPE, ARBAE and MAE. Each group contains three types of maturities. The main results for all futures and options are shown in the top two panels, and the options are divided into different moneyness levels in the lower panels. In the general, FSV-type models show the best in-sample performance, capable of fitting market prices as well as producing volatility skew. Then, 3/2-SVJ demonstrates competitive performance, in consideration of its fewer parameters requirements and good qualifying performance especially in ITM option.

The futures pricing errors and pairwise model comparisons are shown in Panel A of Table 5: the FSV-type models have in-sample APRE of 0.66–0.67, while the 3/2-SVJ model and HSV model respectively obtain 0.8 and 3.55 ARPE. Due to the fact that both FSV-type and 3/2-SVJ have lower ARPE, we turn to verify the MAE metrics which suggest that the futures pricing performance of the FSV-type model is slightly better than other models in the in-sample test. Given the fact that 3/2-SVJ has less parameters than FSV-type, we would like to draw the conclusion that 3/2-SVJ performs better than FSV-type for in-sample pricing futures.

With respect to options, the pricing errors and pairwise model comparisons are shown in Panel B–E of Table 5. From total statistics of each panel, the FSV-type

Table 5 Pricing performances across different models: In-sample

	ARPE				ARBAE				MAE			
	Short	Middle	Long	Total	Short	Middle	Long	Total	Short	Middle	Long	Total
Panel A: All future												
HSV	0.91	2.07	4.45	3.55	N/A	N/A	N/A	N/A	0.16	0.41	0.94	0.74
3/2-SVJ	2.32	0.85	0.55	0.80	N/A	N/A	N/A	N/A	0.41	0.16	0.11	0.16
FSV-AJ	0.63	0.52	0.73	0.66	N/A	N/A	N/A	N/A	0.11	0.10	0.15	0.13
FSV-DJ	0.66	0.46	0.73	0.67	N/A	N/A	N/A	N/A	0.12	0.09	0.16	0.14
Panel B: All options												
HSV	13.91	14.5	17.02	15.07	9.29	11.95	13.94	11.41	0.68	0.84	0.84	0.77
3/2-SVJ	7.97	8.07	16.02	10.65	3.95	5.84	12.97	7.35	0.37	0.35	0.57	0.43
FSV-AJ	6.43	8.35	6.30	6.81	2.91	5.90	3.64	3.81	0.37	0.39	0.29	0.35
FSV-DJ	7.56	8.61	5.78	7.21	3.59	6.16	3.28	4.06	0.44	0.41	0.26	0.37
Panel C: OTM options ($d < -0.1$)												
HSV	40.24	14.89	14.01	15.38	33.76	12.34	10.56	11.97	0.98	0.40	0.45	0.46
3/2-SVJ	26.6	16.01	20.07	19.53	20.60	13.41	16.54	16.08	0.65	0.41	0.56	0.54
FSV-AJ	13.90	13.68	6.05	7.98	7.49	11.07	3.09	4.93	0.33	0.36	0.18	0.22
FSV-DJ	13.77	14.00	5.53	7.76	7.29	11.44	2.78	4.77	0.33	0.37	0.16	0.21
Panel D: ATM options ($-0.1 \leq d \leq 0.1$)												
HSV	23.01	8.40	17.40	17.46	17.12	5.42	14.64	13.30	0.71	0.35	0.87	0.67
3/2-SVJ	8.42	4.00	5.09	6.23	3.83	1.76	2.69	2.94	0.26	0.17	0.26	0.24
FSV-AJ	6.02	6.41	4.20	5.55	2.17	3.60	1.93	2.47	0.18	0.24	0.20	0.20
FSV-DJ	6.18	6.20	3.81	5.45	2.43	3.43	1.64	2.44	0.19	0.23	0.18	0.20

Table 5 continued

	ARPE				ARBAE				MAE			
	Short	Middle	Long	Total	Short	Middle	Long	Total	Short	Middle	Long	Total
Panel E: ITM options (0.1 < d)												
HSV	10.91	16.85	29.45	14.09	6.70	14.40	27.63	10.46	0.66	1.27	2.50	0.98
3/2-SVJ	7.17	5.44	10.35	7.11	3.35	3.42	8.67	3.90	0.37	0.39	0.91	0.43
FSV-AJ	6.24	6.27	9.57	6.58	2.89	4.05	7.76	3.62	0.41	0.47	0.83	0.47
FSV-DJ	7.63	6.08	8.96	7.55	3.70	4.43	7.15	4.20	0.49	0.50	0.77	0.52

This table shows the in-sample performance metrics across the different models. The metric ARPE reports the average pricing error in per cent. The metric ARBAE measures the average error of model prices that fall outside the bid-ask spread. The metric MAE stands for the sample average absolute difference between the market price and the model price. The ARPE and ARBAE performance measures are reported in percentages. The moneyness is defined as $d = VIX/K$ and K is the strike of option contract. Short-term contracts are those with no more than one month to maturity, middle-term contracts are those not only more than one month but also no more than three months to maturity and long-term contracts are those more than three months to maturities

models show better in-sample performance than other models. Every error measures between FSV-AJ and FSV-DJ is getting close, indicating the critical modeling features of free stochastic volatility. The FSV-type models have an in-sample ARPE 6.81–7.21, while the 3/2-SVJ model and HSV model have an in-sample ARPE 10.65 and ARPE 15.07. In addition, FSV-type model has an in-sample ARBAE of 3.81–4.06, while 3/2-SVJ and HSV models have an in-sample ARBAE of 7.35 and 11.41 respectively, larger than those of FSV-type models. It can be concluded that FSV-type shows the lowest average error of model prices falling outside the bid-ask spread. Finally, regarding the reported ARPE value in Panel C, we find that 3/2-SVJ is not appropriate to price OTM options.

Now that the in-sample fit appears to have an increasingly better performance along with HSV, 3/2-SVJ, FSV-DJ and FSV-AJ, one may argue that the outcome can be biased, due to the larger number of parameters and the over-fitting to the data. Moreover, a model that performs well in fitting option prices may have poor predictive qualities. Addressing these concerns, we design the out-of-sample test by using the parameters estimated in Table 4 as inputs to compute the model-based option prices on March 21, 2016 to March 31, 2016, and report the corresponding pricing errors in Table 6. As for futures, the pricing errors and pairwise model comparisons are shown in Panel A of Table 6. The FSV-AJ model has an out-of-sample ARPE of 2.76, while the 3/2-SVJ and HSV models have out-of-sample ARPE 3.02 and 5.59 respectively. With regard to options, the pricing errors and pairwise model comparisons are shown in Panel B–H of Table 6. In total, the FSV-type models have an out-of-sample ARPE of 8.86–9.97, while the 3/2-SVJ and HSV models have14.05 and 16.17. Although 3/2-SVJ does not perform well in pricing OTM options, it is good at pricing ITM options. According to those results, FSV-type models show best out-of-sample performance, capable of generating fewer pricing errors in both futures and options, with competitive 3/2-SVJ model in pricing ITM options. Finally, it can be learned from ARBAE that FSV-AJ shows the lowest average error of model prices falling outside the bid-ask spread.

To further gauge and analyze the effects of including FSV parameter α on pricing futures and options, we now focus on investigation and comparison between FSV-type models with 3/2-SVJ and HSV models. In light of futures, the FSV-AJ model has in-sample ARPE of 0.66 and out-of-sample ARPE of 2.76, while both 3/2-SVJ and HSV cannot fit the market future price quite well. The in-sample MAE metrics of FSV-type models never exceed 0.14, which is lower than the MAE of any other models. Taking a closer look at the short maturities, we find FSV-type models always present better performance, suggesting that the flexible FSV parameter α can leverage on fitting frequently fluctuating the volatility, due to short maturities. To get a capacity sense of each model capturing future price, we plot those of the VIX future values as a function of time to maturities under FSV-AJ, FSV-DJ, 3/2-SVJ and HSV models, and present in Fig. 4. VIX futures are computed by using parameters values given in Table 4. Here time to maturities presented in Fig. 4 are not annualized. All of these indicate that the futures pricing performance of FSV-type models are better than that of the 3/2-SVJ and HSV models, showing the importance of including free stochastic volatility.

Table 6 Pricing performances across different models: Out-of-sample

	ARPE				ARBAE				MAE			
	Short	Middle	Long	Total	Short	Middle	Long	Total	Short	Middle	Long	Total
Panel A: All future												
HSV	4.79	3.33	6.52	5.59	N/A	N/A	N/A	N/A	0.78	0.61	1.31	1.09
3/2-SVJ	8.50	2.95	2.09	3.02	N/A	N/A	N/A	N/A	1.39	0.54	0.42	0.56
FSV-AJ	5.51	3.33	2.09	2.76	N/A	N/A	N/A	N/A	0.94	0.63	0.41	0.52
FSV-DJ	2.68	2.49	4.96	4.14	N/A	N/A	N/A	N/A	0.45	0.46	1.00	0.81
Panel B: All options												
HSV	6.71	16.33	17.23	16.17	3.16	13.93	12.58	12.42	0.41	0.93	1.03	0.95
3/2-SVJ	1.24	12.64	16.52	14.05	0	10.60	12.46	10.92	0.08	0.46	0.55	0.48
FSV-AJ	7.14	10.82	7.82	8.86	2.86	8.44	4.19	5.65	0.45	0.48	0.42	0.45
FSV-DJ	12.92	13.86	7.10	9.97	8.20	11.42	4.01	7.00	0.82	0.57	0.33	0.45
Panel C: OTM options (d ≤ −0.1)												
HSV	N/A	21.86	10.37	12.92	N/A	18.71	5.49	8.43	N/A	0.56	0.39	0.43
3/2-SVJ	N/A	33.34	24.83	26.72	N/A	30.06	19.39	21.77	N/A	0.89	0.75	0.78
FSV-AJ	N/A	22.13	6.20	9.74	N/A	18.85	2.22	5.92	N/A	0.60	0.20	0.29
FSV-DJ	N/A	28.96	7.69	12.42	N/A	25.68	4.21	8.98	N/A	0.80	0.24	0.36
Panel D: ATM options (−0.1 < d < 0.1)												
HSV	N/A	7.83	24.49	18.05	N/A	5.46	19.62	14.15	N/A	0.41	1.52	1.09
3/2-SVJ	N/A	8.81	3.86	5.77	N/A	6.76	1.88	3.77	N/A	0.42	0.22	0.30
FSV-AJ	N/A	7.04	8.30	7.82	N/A	4.63	5.03	4.88	N/A	0.33	0.53	0.45
FSV-DJ	N/A	12.31	4.83	7.72	9.75	2.29	5.17	2.44	N/A	0.59	0.30	0.41

Table 6 continued

Panel E: ITM options (0.1 ≤ d)

	ARPE				ARBAE				MAE			
	Short	Middle	Long	Total	Short	Middle	Long	Total	Short	Middle	Long	Total
HSV	6.71	17.24	33.00	19.21	3.16	15.25	29.61	16.54	0.41	1.38	2.77	1.54
3/2-SVJ	1.24	3.20	3.19	2.80	0	1.84	1.35	1.33	0.08	0.24	0.26	0.21
FSV-AJ	7.14	6.44	13.38	8.39	2.86	4.56	10.58	5.79	0.45	0.49	1.13	0.65
FSV-DJ	12.92	6.40	8.24	8.20	8.20	4.48	5.84	5.59	0.82	0.45	0.70	0.59

This table shows the out-of-sample performance metrics across the different models. The metric ARPE reports the average pricing error in per cent. The metric ARBAE measures the average error of model prices that fall outside the bid-ask spread. The metric MAE stands for the sample average absolute difference between the market price and the model price. The ARPE and ARBAE performance measures are reported in percentages. The moneyness is defined as $d = $ VIX$/K$ while K is the strike of option contract. Short-term contracts are those with less than one month to maturity, middle-term contracts are those between one-to-three months to maturity, and long-term contracts are those more than three months to maturities
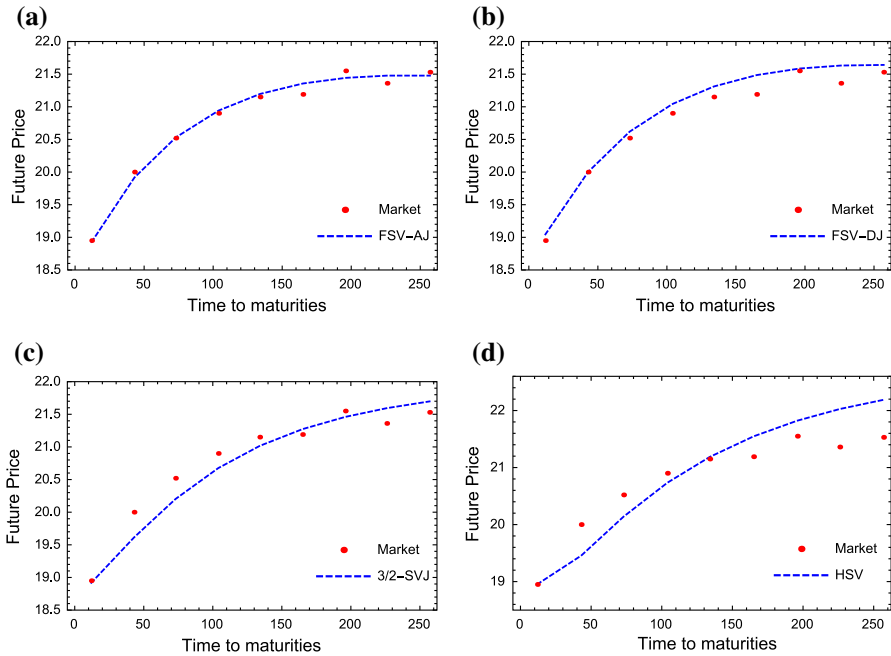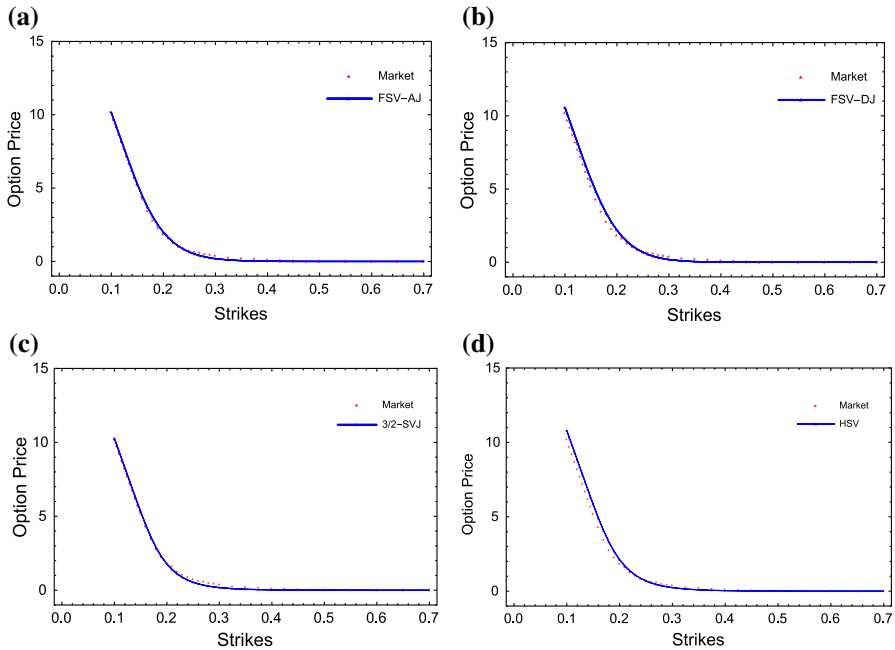
Fig. 4 Graph of the VIX futures price as a function of time to maturities (days). VIX futures are computed by four models with regard to 9 different maturities, using the parameters estimated in Table 4. **a** FSV-AJ, **b** FSV-DJ, **c** 3/2-SVJ, **d** HSV

With regard to options, we separate option pricing errors into maturities and several moneyness. The FSV-type models have in-sample ARPE of 6.81–7.21 and MAE of 0.35–0.37, while 3/2-SVJ model has in-sample ARPE of 10.65 and MAE of 0.43. HSV model perform not quite well in pricing options, having in-sample ARPE of 15.07 and MAE of 0.77. Based on Panel C of in-sample and out-of-sample presented in Tables 5 and 6, we conclude that FSV-type models greatly improve the pricing of OTM options, especially in comparison with 3/2-SVJ model.

For the ITM options presented in Panel E of Table 6, all the models except 3/2-SVJ generate larger percentage errors in the ITM options of out-of-sample test, showing that 3/2-SVJ is quite competent in ITM options pricing with the advantage of its less parameters and simplicity. To get a capability sense of each model capturing option price, we plot those of the VIX option value as a function of 38 strikes, from 10 to 70, under time to maturities 28 days, and present them in Fig. 5. FSV-type models outperform the other models in OTM options while 3/2-SVJ literally has a decent performance in ITM options. After comparing all in-sample ARPE with out-of-sample ARPE in each model, FSV-type models perform more stably in pricing futures and options than any other models. To sum up, including free volatility parameter α in our model plays a crucial role in fitting the prices of futures and options.

Lastly, we evaluate the incremental effect of upward and downward jumps on the pricing of futures and options. Now we eye on the FSV-AJ and FSV-DJ pricing errors. Panels A–E of Tables 5 and 6 show the in-sample and out-of sample ARPE and MAE.

Fig. 5 Graph of the VIX option price as a function of strikes. VIX options are computed by four models with respect to 38 strikes, using the parameters estimated in Table 4. Here the strikes are divided by 100. **a** FSV-AJ, **b** FSV-DJ, **c** 3/2-SVJ, **d** HSV

On the whole, FSV-AJ shows the better in-sample and out-of-sample performance in futures and OTM options.

Heuristically, it seems that including upward jump in FSV-AJ contribute to decreasing VIX so as to make OTM options back to ITM options. Hence, FSV-AJ performs decently in OTM options pricing. It also can be seen in Fig. 5 that FSV-AJ is closer to market prices at lower strike ahead of 20. Although the FSV-AJ model greatly improves the pricing of OTM call options in out-of-sample tests, there is no significant pricing differences between the FSV-AJ and FSV-DJ, considering the pricing of in-sample futures, options and out-of-sample ITM options. A conclusion could be drew that including upward jumps cannot be rejected in the case that free stochastic volatility and downward jumps have been taken into consideration already.

8 Conclusion

In this paper, we have introduced an efficient and flexible model, FSV model, an extension of the celebrated Heston model and 3/2 plus jumps model in an unified framework by preserving the analytical tractability. We initiate in deriving and establishing the quasi-closed form solution for VIX future and call option price. The models have three innovative features which are completely different from those previous ones addressed in literature. Firstly, we free the power parameter α of instantaneous variance of CIR

process, instead of fixing α. Thus, we free FSV parameters α, allowing the data to voice its authentic direction. In addition to Feller condition, we also add non-explosion condition $\frac{2\kappa\theta}{\sigma^2} > 1 - \alpha$ and succeed in proving that the discounted price stock is a true martingale. Secondly, for the first time, our paper testifies that FSV-type models can be closer to the practical dynamics of S&P500 by using GMM technique as test. Results show that α of the indices can present different volatility fluctuations in corresponding periods. In other words, another subclass of FSV-type is preferred and the newly added α can assist in agilely capturing the equity distribution.Thirdly, instead of bundling upward and downward jumps together in a normal distribution, we separate them in equity to better consider the fact that investors react differently to good and bad shocks.

According to the in-sample measure and out-of-sample forecast, adding the FSV parameter α and jumps features to the model can greatly improve its performance, especially in pricing OTM options. Model with jumps outperforms in pricing performance, and we find that upward jumps owns more crucial features in pricing OTM option. Though all of the models perform decently in capturing the decreasing pattern in the implied volatility, only FSV-AJ and FSV-DJ models could succeed in matching the flat pattern in the implied skewness, which is consistent with the results that FSV parameter α and jumps are equally important for pricing the VIX derivatives.

Finally, this paper has several works remaining to be discussed for which we hope to capitalize in future. For instance, it is unknown the ability of FSV-type models to jointly price of S&P500 option and realized-variance derivatives. Furthermore, Fourier cosine series expansions and characteristic function of underlying asset return process are expected to be provided so as to hedge European-style options in discrete time. Adding jumps in instantaneous variance process is worthy further exploration. All of these topics deserve to be attached with close attention, and be the our future research concentration.

Appendix: Derivation of 1st and 2nd order moment of ε_{t+1}

To derive $\mathbb{E}^{\mathbb{Q}}[\varepsilon_{t+1}]$ and $\mathbb{E}^{\mathbb{Q}}[\varepsilon_{t+1}^2]$, we split the Brownian motion $W^{\mathbb{P}}$ into $Z^{\mathbb{P}}$ and its orthogonal part $Z^{\mathbb{P},\perp}$ and obtain

$$
\begin{aligned}
\varepsilon_{t+1} &= \delta_s^* V_{t+1} \Delta t + \gamma^* V_{t+1}^\alpha W^{\mathbb{P}}(\Delta t) \\
&= \delta_s^* V_{t+1} \Delta t + \gamma^* V_{t+1}^\alpha \left[\rho Z^{\mathbb{P}}(\Delta t) + \sqrt{1-\rho^2} Z^{\mathbb{P},\perp}(\Delta t) \right].
\end{aligned}
$$

Taking expectation to both sides, it follows that

$$
\begin{aligned}
\mathbb{E}_t[\varepsilon_{t+1}] &= \delta_s^* \mathbb{E}_t[V_{t+1}] \Delta t + \rho\gamma^* \mathbb{E}_t \left[V_{t+1}^\alpha Z^{\mathbb{P}}(\Delta t) \right] \\
&\quad + \gamma^* \sqrt{1-\rho^2} \mathbb{E} \left[V_{t+1}^\alpha Z^{\mathbb{P},\perp}(\Delta t) \right]
\end{aligned}
$$

$$
\begin{aligned}
&= \delta_s^* \mathbb{E}_t[V_{t+1}] \Delta t + \rho \gamma^* \mathbb{E}_t \left[V_{t+1}^\alpha \right] * \mathbb{E}_t \left[Z^{\mathbb{P}}(\Delta t) \right] \\
&\quad + \gamma^* \sqrt{1 - \rho^2} \mathbb{E} \left[V_{t+1}^\alpha \right] * \mathbb{E} \left[Z^{\mathbb{P}, \perp}(\Delta t) \right] \\
&= \delta_s^* \Delta t \, G(\kappa^*, \theta^*, \sigma, -1; \Delta t, V_t).
\end{aligned}
$$

The second and third terms in the last equation equal 0 due to the independence and independent increments of Brownian motion. On the other hand, the second moment of ε_{t+1} is explicitly known as

$$
\begin{aligned}
\mathbb{E}[\varepsilon_{t+1}^2] &= \mathbb{E}_t \left[\delta_s^{*2} V_{t+1}^2 \Delta t^2 + \gamma^{*2} V_{t+1}^{2\alpha} (W^{\mathbb{P}}(\Delta t))^2 + 2\delta_s^* \Delta t \gamma^* V_{t+1}^{\alpha+1} W^{\mathbb{P}}(\Delta t) \right] \\
&= \delta_s^{*2} \Delta t^2 \phi(\Delta t, V_t; -2, 0, 0, 0) + \mathbb{E}_t \left[\gamma^{*2} V_{t+1}^{2\alpha} (\rho Z^{\mathbb{P}}(\Delta t) + \sqrt{1 - \rho^2} Z^{\mathbb{P}, \perp}(\Delta t))^2 \right] \\
&= \delta_s^{*2} G(\kappa^*, \theta^*, \sigma, -2; \Delta t, V_t) \Delta t^2 + \gamma^{*2} G(\kappa^*, \theta^*, \sigma, -2\alpha; \Delta t, V_t) \Delta t
\end{aligned}
$$

where we use Remark 2.1 by setting η to be different values and the fact that V_t is a Markov process.

References

Bates, D. S. (2000). Post-'87 crash fears in the S&P 500 futures option market. *Journal of Econometrics*, *94*(1–2), 181–238.

Baldeaux, J., & Badran, A. (2014). Consistent modelling of VIX and equity derivatives using a 3/2 plus jumps model. *Applied Mathematical Finance*, *21*(4), 299–312.

Bluman, G., & Kumei, S. (1989). *Symmetries and differential equations*. Applied Mathematical Sciences, Vol. 81. New York: Springer.

Breeden, D. T., & Litzenberger, R. H. (1978). Prices of state-contingent claims implicit in option prices. *Journal of Business*, *51*(4), 621–651.

CBOE. (2003). VIX: CBOE volatility index. Available at www.cboe.com/micro/vix/vixwhite.pdf.

Chan, K. C., Karolyi, G. A., Longstaff, F. A., & Sanders, A. B. (1992). An empirical comparison of alternative models of the short-term interest rate. *The Journal of Finance*, *47*(3), 1209–1227.

Craddock, M., & Lennox, K. A. (2009). The calculation of expectations for classes of diffusion processes by Lie symmetry methods. *The Annals of Applied Probability*, *19*(1), 127–157.

Drimus, G. G. (2012). Options on realized variance by transform methods: A non-affine stochastic volatility model. *Quantitative Finance*, *12*(11), 1679–1694.

Duan, J. C., & Yeh, C. Y. (2010). Jump and volatility risk premiums implied by VIX. *Journal of Economic Dynamics and Control*, *34*(11), 2232–2244.

Goard, J., & Mazur, M. (2013). Stochastic volatility models and the pricing of VIX options. *Mathematical Finance*, *23*(3), 439–458.

Grasselli, M. (2017). The 4/2 stochastic volatility model: A unified approach for the Heston and the 3/2 model. *Mathematical Finance*, *27*(4), 1013–1034.

Grunbichler, A., & Longstaff, F. A. (1996). Valuing futures and options on volatility. *Journal of Banking & Finance*, *20*(6), 985–1001.

Hansen, L. P. (1982). Large sample properties of generalized method of moments estimators. *Econometrica*, *50*(4), 1029–1054.

Heston, S. L. (1993). A closed-form solution for options with stochastic volatility with applications to bond and currency options. *Review of Financial Studies*, *6*(2), 327–343.

Lewis, A. L. (2000). *Option valuation under stochastic volatility*. Newport Beach, CA: Finance Press.

Lian, G. H., & Zhu, S. P. (2013). Pricing VIX options with stochastic volatility and random jumps. *Decisions in Economics and Finance*, *36*(1), 71–88.

Lin, W., Li, S. H., Luo, X. G., & Chern, S. (2017). Consistent pricing of VIX and equity derivatives with the 4/2 stochastic volatility plus jumps model. *Journal of Mathematical Analysis and Applications*, *447*(2), 778–797.

Olver, P. J. (1993). *Applications of Lie groups to differential equations*, 2nd Edn. Graduate Texts in Mathematics, 107. New York: Springer.

Pan, J. (2002). The jump-risk premia implicit in options: evidence from an integrated time-series study. *Journal of Financial Economics*, *63*(1), 3–50.

Park, Y. H. (2016). The Effects of asymmetric volatility and jumps on the pricing of VIX derivatives. *Journal of Econometrics*, *192*(1), 313–328.

Sepp, A. (2008). VIX option pricing in a jump-diffusion model. *Risk Magazine*, 84–89. https://papers.ssrn.com/sol3/papers.cfm?abstract_id=1412339.

Whitney, K. N. (1985). Generalized method of moment specification testing. *Journal of Econometric*, *29*, 229–256.

Zhang, J. E., & Zhu, Y. (2006). VIX futures. *Journal of Futures Markets*, *26*(6), 521–531.